

Non-thermal Dark Matter and the Moduli Problem in String Frameworks

Bobby S. Acharya*

*Abdus Salam International Center for Theoretical Physics
Strada Costiera 11, 34014 Trieste. ITALY and
INFN, Sezione di Trieste and
Michigan Center for Theoretical Physics
University of Michigan,
Ann Arbor, Michigan 48109, USA*

Piyush Kumar†

*Department of Physics
University of California, Berkeley, CA 94720, USA and
Theoretical Physics Group
Lawrence Berkeley National Laboratory, Berkeley, CA 94720, USA*

Konstantin Bobkov‡, Gordon Kane§, Jing Shao¶, and Scott Watson||

*Michigan Center for Theoretical Physics
University of Michigan,
Ann Arbor, Michigan 48109, USA*

ABSTRACT: We address the cosmological moduli/gravitino problems and the issue of too little thermal but excessive non-thermal dark matter from the decays of moduli. The main examples we study are the G_2 -MSSM models arising from M theory compactifications, which allow for a precise calculation of moduli decay rates and widths. We find that the late decaying moduli satisfy both BBN constraints and avoid the gravitino problem. The non-thermal production of Wino LSPs, which is a prediction of G_2 -MSSM models, gives a relic density of about the right order of magnitude.

*bacharyaATcern.ch

†kpiyush@berkeley.edu

‡bobkov@umich.edu

§gkane@umich.edu

¶jingshao@umich.edu

||watsongs@umich.edu

Contents

1. Introduction	2
2. Early Universe Cosmology in the Presence of Moduli	3
2.1 Addressing the “Overshoot Problem”	4
3. Overview of Results	5
3.1 Scalar Decay and Reheating Temperatures	7
3.1.1 Moduli decay and BBN	8
4. Summary of Results for the G_2-MSSM	8
4.1 Moduli Masses	10
4.2 Couplings and Decay Widths	11
4.3 Nature of the LSP	12
5. Evolution of Moduli in the G_2-MSSM	13
5.1 Moduli Oscillations	13
5.2 Moduli Decays and Gravitino Production	13
5.2.1 Heavy Modulus Decay and Initial Thermal Abundances	14
5.2.2 Meson/Light Moduli Decays and the Gravitino Problem	14
6. Dark Matter from the G_2-MSSM	15
6.1 Standard Thermal Dark Matter	15
6.2 Non-thermal Production from Scalar Decay	16
6.2.1 Case one: LSP Yield Above the Fixed Point	17
6.2.2 Case two: LSP Yield Below the Fixed Point	17
6.3 Dark Matter in the G_2 -MSSM	17
7. Discussion of Results	19
8. Summary and Future Directions	21
9. Acknowledgements	23
A. Cosmology of the G_2-MSSM Moduli – A detailed treatment	24
A.1 Heavy modulus oscillations	24
A.2 Meson and Light Moduli Oscillations	25
A.3 Heavy Modulus Decay	25
A.4 Meson Decay	26
A.5 Light Moduli Decays	27
B. Couplings and Decay Widths of the Moduli and Meson Fields	27
B.1 Moduli Couplings	27
B.2 Meson Couplings	31
B.3 RG evolution of the couplings	32
B.4 Decay Rates of the Moduli	33
B.5 Decay Width of the Meson	37

1. Introduction

The existence of Dark Matter seems to require physics beyond the Standard Model. If this physics arises from a string/ M theory vacuum, one is faced with various problems associated with the moduli fields, which are gauge-singlet scalar fields that arise when compactifying string/ M theory to four dimensions. In particular, moduli fields can give rise to disastrous cosmological effects.

For example, the moduli have to be stabilized, or made massive, in accord with cosmological observations. Even if these moduli are made massive, there could be a large amount of energy stored in them leading to the formation of scalar condensates. In most cases, this condensate will scale like ordinary matter and will quickly come to dominate the energy density. The moduli are unstable to decays to photons, and when this occurs, the resulting entropy can often spoil the successes of big-bang nucleosynthesis (BBN). This is the cosmological moduli problem [1–5]. In supersymmetric extensions of the standard model, the overproduction of gravitinos can cause similar problems and have been a source of much investigation [6–19].

In addition, the “standard” picture in which Dark Matter (DM) particles are produced during a phase of thermal equilibrium can be significantly altered in the presence of moduli. The moduli, which scale like non-relativistic matter, typically dominate the energy density of the Universe making it matter dominated. Therefore, the dominant mechanism for production of DM particles is non-thermal production via the direct decay of moduli¹. However, this can lead to further problems since it is easy to produce too much dark matter compared with what we observe today.

In recent years there has been considerable progress in our understanding of moduli dynamics and their potential in different frameworks which arise in various limits of string/ M theory. The most popular examples include the KKL^T and Large Volume frameworks in Type IIB string theory [23–25], where all moduli are stabilized by a combination of fluxes and quantum corrections. These frameworks are also attractive in the sense that they provide a mechanism for supersymmetry breaking at low scales (\sim TeV), thus accommodating the hierarchy between the Electroweak and Planck scales (see [26–28] for reviews). Since one can concretely study the couplings between moduli and matter fields, we have an opportunity to address many issues in particle physics and cosmology from an underlying microscopic viewpoint. The cosmological moduli/gravitino problems and adequate generation of dark matter within the Type IIB frameworks has met with some mixed success in a recent paper [29].

In this paper we will study a different framework, in which we will also address the Dark Matter and moduli/gravitino problems. This is the low energy limit of M theory vacua in which the extra dimensions form a manifold of G_2 holonomy. Although the study of such vacua has proven to be technically challenging, much progress has been made towards understanding the effective four dimensional physics emerging from them [31–34]. This includes many phenomenological implications of these vacua, in particular relating to issues such as constructing a realistic visible sector with chiral matter and non-abelian gauge bosons, supersymmetry breaking, moduli stabilization in a dS vacuum as well as explaining the Hierarchy between the Electroweak and Planck scales, as exemplified in a number of works [30, 35–39].

We will show that the moduli, gravitino and dark matter problems are all naturally solved within this framework. Because of the presence of moduli, the Universe is matter-dominated from the end of inflation to the beginning of BBN. The LSPs are mostly produced non-thermally via moduli decays. The final result for the relic density only depends on the masses and couplings of the lightest of the moduli (which decay last) and the mass of the LSP. This is related to the fact that the LSP is a Wino in the G_2 -MSSM and that there is a fairly model independent critical LSP density at freeze out. For natural/reasonable choices of microscopic parameters defining the G_2

¹For other phenomenologically based approaches to non-thermal dark matter and the related issue of baryon asymmetry in the presence of scalar decay see [20–22].

framework, one finds that it is possible to obtain a relic density of the right order of magnitude (up to factors of $\mathcal{O}(1)$). With a more sophisticated understanding of the microscopic theory, one might obtain a more precise result. The qualitative features which are crucial in solving the above problems may also be present in other realistic string/ M theory frameworks.

Moduli which decay into Wino LSPs have been considered previously in the context of Anomaly Mediated Supersymmetry Breaking Models (AMSB) by Moroi and Randall [40]. The moduli and gaugino masses they consider are qualitatively similar to those of the G_2 -MSSM. There are some important differences however. In particular, the MSSM scalar masses in the [40] are much lower than the G_2 -MSSM, leading to much fewer LSPs produced per modulus decay compared to the G_2 models. Furthermore, unlike in AMSB, in the G_2 case one is able to calculate all the moduli masses and couplings explicitly which leads to a more detailed understanding. In essence, though, many of the important ideas in our work are already present in [40]. The G_2 -MSSM models can be thought of as a concrete microscopic realization of the relevant qualitative features of the AMSB models.

Interestingly, our actual result for the relic density (equation 6.17) is a few times larger than the WMAP value if we use central values for the microscopic constants, which should probably be regarded as a success. It is also worth remarking that, contrary to common views, it is not at all possible to get any value one wants – we can barely accommodate the actual observed value in the G_2 framework.

The paper is organized as follows. In Section 2 we briefly summarize early universe cosmology in the presence of moduli, and address many of the issues associated with their stabilization and decay. In Section 3 we give a non-technical overview of the main results. This is largely because much of this paper involves technical calculations. In section 4 we present a brief review of the G_2 -MSSM, a model which arises after considering moduli stabilization within the framework of M theory compactifications. A basic discussion of decay rates and branching ratios for the moduli and gravitinos in this model follows, with a detailed calculation left for Appendix B. Then in section 5, we consider again the cosmology of moduli presented in section 2) for the case of the G_2 -MSSM. In section 6, after a review of dark matter production in both the thermal and non-thermal cases, we consider the dark matter abundance arising from the non-thermal decay of the G_2 -MSSM moduli. This section is a more technical overview of the salient features of dark matter production, leaving an even more detailed treatment for Appendix A. In this section we present our main result, which is that the G_2 -MSSM naturally predicts a relic density of Wino-like neutralinos of about the right magnitude in agreement with observation. This is followed by a detailed discussion of the results obtained and how it depends on the qualitative (and quantitative) features of the underlying physics. We then conclude with considerations for the future.

2. Early Universe Cosmology in the Presence of Moduli

Before considering the particular case of moduli in the G_2 -MSSM, we first briefly review the early universe evolution of moduli and the associated cosmological issues that can result. This section will also serve to set our conventions.

Currently, the only convincing model leading to a smooth, large, and nearly isotropic Universe as well as providing a mechanism for generating density perturbations for structure formation is cosmological inflation. At present we have very little understanding of how the “inflationary era” might arise within the M theory framework. In what follows, therefore, we will assume that adequate inflation and (p)reheating have taken place and focus on the post-reheating epoch. We will also conservatively take the inflationary reheat temperature to be near the unification scale $10^{14} - 10^{15}$ GeV, so that possibilities for high-scale baryogenesis exist. We will comment more on this issue at the end.

During inflation, the moduli fields are generically displaced from their minima by an amount of $\mathcal{O}(m_p)$ [41]. This can be seen by looking at the following generic potential experienced by the moduli:

$$V(\psi) \sim \frac{1}{2}m_{soft}^2(\psi - \psi_0)^2 - H_{inf}^2(\psi - \psi_0)^2 + \frac{1}{m_p^{2n}}(\psi - \psi_0)^{4+2n} \quad (2.1)$$

where ψ_0 is the true vacuum-expectation-value (vev) of the field, i.e. in the present Universe. Only the first term in (2.1) comes from zero-temperature supersymmetry breaking, the other two highlight the importance of high-scale corrections and the mass-squared parameter ($\sim -H_{inf}^2$) which results from the finite energy density associated with cosmological inflation [41]. As argued earlier, the potential (2.1) is dominated by the last two terms during inflation since $H_{inf} \gg m_{soft} \sim m_{3/2}$. Thus, a minimum of the potential will occur near:

$$\langle \psi \rangle_{inf} \sim \psi_0 + m_p \left(\frac{H_{inf}}{m_p} \right)^{1/(n+1)} \quad H \gg m_{soft}. \quad (2.2)$$

Here, for simplicity, we have implicitly assumed that the induced mass-squared parameter for ψ during inflation is *negative* and of $\mathcal{O}(H_{inf}^2)$. This is possible for a non-minimal coupling between the inflationary fields and the moduli, a generic possibility within string theory. A large displacement of moduli fields is also possible when the induced mass-squared parameter during inflation is positive, but much smaller than $|H_{inf}^2|$. In this case, large dS fluctuations can drive the moduli fields to large values during inflation. Therefore, independent of details, the assumption we make is that gauge singlet scalar fields like moduli (and meson fields in the G_2 -MSSM) will be displaced from their present minimum by large values.

After the end of inflation and subsequent cosmological evolution, when $H \lesssim m_{3/2}$, the soft mass term in the potential will dominate and we have:

$$\langle \psi \rangle_{present} \sim \psi_0 \quad H \lesssim m_{soft}. \quad (2.3)$$

ψ_0 is also typically of order m_p . In Section 4, we will present the soft masses and decay rates for the moduli arising from soft SUSY breaking in the G_2 -MSSM low-energy effective theory relevant in the present Universe. Thus, we see that by considering moduli in the early universe with high-scale inflation, it is a rather generic consequence to expect moduli to be displaced from their low-energy (present) minimum by an amount:

$$|\Delta\psi| \equiv |\langle \psi \rangle_{inf} - \langle \psi \rangle_{present}| \approx m_p \left(\frac{H_{inf}}{m_p} \right)^{1/(n+1)} \lesssim m_p \quad (2.4)$$

2.1 Addressing the ‘‘Overshoot Problem’’

The evolution of moduli after the end of inflation is governed by the following equation:

$$\ddot{\psi} + (3H + \Gamma_\psi)\dot{\psi} + \frac{\partial V}{\partial \psi} = 0. \quad (2.5)$$

where the modulus decay rate $\psi \rightarrow XX$ is given by:

$$\Gamma_\psi = D_\psi \frac{m_\psi^3}{m_p^2}, \quad (2.6)$$

which reflects the fact that the modulus is gravitationally coupled ($\Gamma_\psi \sim G_N \sim m_p^{-2}$) and D_ψ is a model dependent constant that is typically order unity. After the end of inflation, the Universe is dominated by coherent oscillations of the inflaton field and $H \sim \frac{2}{3t}$. After the decay of the inflaton

and subsequent reheating at temperature T_r , the Universe is radiation dominated and $H \sim \frac{1}{2t}$. In both these phases, the evolution of the moduli can be written as:

$$\ddot{\psi} + \mathcal{O}(1)\frac{1}{t}\dot{\psi} + \frac{\partial V}{\partial \psi} = 0. \quad (2.7)$$

where we have neglected Γ_ψ as it is planck suppressed. The minimum of the potential now is *time-dependent* due to the time dependence of the Hubble parameter. The evolution of the moduli in the presence of matter and/or radiation as in the case above, has been studied in [42–51]. In this case, as the modulus begins to roll down the potential, it was shown in [42, 45–47]) that the presence of matter/radiation has a slowing effect on the evolution of the field. This can naturally allow for the relaxation of moduli into coherent oscillations about the time-dependent minimum². This ‘environmental relaxation’ can then slowly guide the modulus to the time-dependent minimum.

Another possibility arises if the minimum of the potential is located at a point of enhanced symmetry where additional light degrees of freedom become important. This naturally arises in SUGRA theories that are derived from string theories, where an underlying knowledge of the UV physics is known [49, 50, 52, 53]. If the modulus initially has a large kinetic energy, as it evolves close to the point of enhanced symmetry, new light degrees of freedom will be produced and then backreact to pull the modulus back to the special point of enhanced symmetry. This simple example of ‘moduli trapping’ is present in a large number of examples in string theory with points of enhanced symmetry [48–51].

The above effects lead to a natural solution of the so-called ‘overshoot problem’ [54] (see also [55]), as argued below. As the universe expands and cools, the Hubble parameter (H) decreases until it eventually drops below the mass of the modulus m_ψ ($\sim m_{3/2}$). Thus, from (2.1), we see that the first term in the potential now becomes of the same order as the other two terms and can no longer be neglected. At this time the modulus field becomes under-damped and begins to oscillate freely about the true minimum ψ_0 with amplitude $f_\psi \sim (m_p^n m_\psi)^{1/(n+1)}$. As an example, for $n = 1$, f_ψ is $(m_p m_\psi)^{1/2}$ leading to a potential value $V \sim m_\psi^2 f_\psi^2 \sim m_\psi^3 m_p$ which is much smaller than the overall height of the potential barrier at this time ($\sim m_\psi^2 m_p^2$, as in any soft susy breaking potential). Thus, there is no overshoot problem.

The modulus will now quickly settle into coherent oscillations at a time roughly given by $t_{osc} = 2H^{-1} \sim 2m_\psi^{-1}$. After coherence is achieved, the scalar condensate will then evolve as pressure-less matter³, i.e. $\rho_m(t_{osc}) = \frac{1}{2}m_\psi^2 f_\psi^2$. Because the condensate scales as pressure-less matter $\rho_m \sim 1/a^3$, its contribution relative to the background radiation $\rho_r \sim 1/a^4$ will grow with the cosmological expansion as $a(t) \sim 1/T$. Thus, if enough energy is stored initially in the scalar condensate it will quickly grow to dominate the total energy density.

3. Overview of Results

This section reviews the main results of the paper without technical details.

As explained above, the moduli start oscillating when the Hubble parameter drops below their respective masses. Then they eventually dominate the energy density of the Universe before decaying. Within the context of G_2 -MSSM models, the relevant field content is that of the MSSM and $N + 1$ real scalars. N of these are the moduli, X_K , of the G_2 -manifold and the remaining one is a scalar field, ϕ , called the meson field, which arises in the hidden sector dominating the supersymmetry breaking. A reasonable choice for N would be $\mathcal{O}(50) - \mathcal{O}(100)$.

²We thank Joe Conlon and Nemanja Kaloper for discussions on this approach.

³If there are additional terms that contribute to the potential (besides the soft mass), then a coherently oscillating scalar does not necessarily scale as pressure-less matter.

The masses are roughly as follows. The lightest particles beyond the Standard Model particles are the gauginos. In terms of the gravitino mass, $m_{3/2}$, their masses are of order $\kappa m_{3/2}$, suppressed by a small number κ . κ is determined by a combination of tree level and one-loop contributions which turn out to be comparable. The tree-level contribution is suppressed essentially because ϕ dominates the supersymmetry breaking, and to leading order, the gauge couplings are independent of ϕ . The precise spectrum of gaugino masses is qualitatively similar, but numerically different, to AMSB models. The LSP is a Wino in the G_2 -MSSM, similar to AMSB models. The current experimental limits on gauginos require that the gravitino mass is at least 10 TeV or so. In the G_2 framework, gravitinos naturally come out to be of $\mathcal{O}(10 - 100)$ TeV [38]. 50 TeV is a typical mass that we consider in this paper. The MSSM sfermions and higgsinos have masses of order $m_{3/2}$, except the right handed stop which is a factor of few lighter due to RG running. Of the N moduli, one, X_N is much heavier than the rest, X_i . The heavy modulus mass is about 600 $m_{3/2}$, while the $(N - 1)$ light moduli are essentially degenerate with masses $\sim 2m_{3/2}$. Finally the meson mass is also about $2m_{3/2}$. The decays of the moduli and meson into gravitinos will therefore be dominated by the heavy modulus X_N .

The decays can be parameterized by the decay width as,

$$\Gamma_X = D_X \frac{m_X^3}{m_p^2} \quad (3.1)$$

reflecting the fact that the decays are gravitationally suppressed. D_X is a constant which we calculate to be order one for the moduli but order 700 for ϕ . So, the light moduli have decay widths of order 10^{-13} eV, corresponding to a lifetime of order 10^{-3} s. The heavier scalars have shorter lifetimes, 10^{-5} s for ϕ and 10^{-10} for X_N , see tables 1 and 2. So, as the Universe cools further and H reaches a value of order Γ_{X_N} , the heavy modulus decays. When this happens, the Universe is reheated to a temperature, roughly of order $T_r \sim (\Gamma_{X_N}^2 m_p^2)^{1/4} \sim 40$ GeV. The entropy is increased in this phase, by a factor of about 10^{10} . This greatly dilutes the thermal abundance of gravitinos and MSSM particles produced during reheating (by the inflaton). The abundance of the light moduli and meson are also diluted. Then, when H reaches order Γ_ϕ the meson decays. This reheats the Universe to a temperature $T_r \sim 100$ MeV and increases the entropy by a factor of order 100. Finally, as the Universe cools again and reaches a temperature of about 10^{-13} eV the light moduli decay. They reheat the Universe to a temperature of about 30 MeV and a dilution factor of about 100 again. After this, all the moduli have decayed and the energy density is dominated by the decay of the light moduli. Since the final reheat temperature is well above that of nucleosynthesis, BBN can occur in the standard way.

Furthermore, since the entropy increases by a total factor of about 10^{14} , the gravitino density produced by moduli and meson decays is sufficiently diluted to an extent that it avoids existing bounds from BBN from gravitino decays.

Since the energy density is dominated by the decaying light moduli, the relic density of Wino LSP's is dominated by this final stage of decay. The initial density of LSP's at the time of production is such that the expansion rate is not large enough to prevent self-interactions of LSP's. This is because

$$n_{LSP}^{initial} > \left. \frac{3H}{\langle \sigma v \rangle} \right|_{T_r} \quad (3.2)$$

where the right side is to be evaluated at the final reheating temperature and σv is the typical Wino annihilation cross-section $\sim 10^{-7}$ GeV $^{-2}$. Therefore, the Wino's will annihilate until they reach the density given on the R.H.S., which is roughly 10^{12} eV 3 - an energy density of 10^{23} eV 4 . Here we have assumed, as is reasonable, that since there is a lot of radiation produced at the time of decay, the LSPs quickly become non-relativistic by scattering with this 'background'. Since the entropy at the time of the last reheating $s \sim 10 T^3 \sim 10^{23}$ eV 3 , the ratio of the energy density to entropy,

is around 1 eV. This should be compared to the observed value of this ratio today, which is $3.6 h^2$ eV, where the Hubble parameter today is about 0.71.

Therefore, we see that the Wino LSP relic density is very reasonable in these models. The rest of this paper is devoted to a much more precise, detailed version of this calculation.

3.1 Scalar Decay and Reheating Temperatures

Here we collect some more precise formulae for the decay and reheat temperatures as a function of the moduli/meson masses.

The temperature at the time of decay can be found using

$$3H_d^2 = \frac{m_\psi Y_\psi}{m_p^2} s_d = \frac{m_\psi Y_\psi}{m_p^2} \left(\frac{2\pi^2}{45} \right) g_{*s}(T_d) T_d^3, \quad (3.3)$$

$$\longrightarrow T_d = \left(\frac{30}{\pi^2} \right)^{1/3} \left(\frac{\Gamma_\psi^2 m_p^2}{m_\psi Y_\psi g_{*s}(T_d)} \right)^{1/3}, \quad (3.4)$$

where $Y_\psi = n_\psi/s$ is the comoving number density and

$$s = \frac{\rho + p}{T} = \frac{2\pi^2}{45} g_{*s} T^3, \quad (3.5)$$

is the entropy density with g_{*s} the number of relativistic degrees for freedom⁴. Parameterizing the decay rate as above, i.e. $\Gamma_\psi = D_\psi m_\psi^3/m_p^2$ we find

$$T_d = \left(\frac{30}{\pi^2} \right)^{1/3} g_{*s}^{-1/3}(T_d) \left(\frac{D_\psi^2 m_\psi^5}{Y_\psi m_p^2} \right)^{1/3} \quad (3.6)$$

For later use we also note that if more than one modulus dominates at the time of decay then the temperature at the time of decay becomes

$$T_d = \left(\frac{30}{\pi^2} \right)^{1/3} g_{*s}^{-1/3}(T_d) \left(\frac{D_\psi^2 m_\psi^6}{m_p^2 \sum_i m_i Y_i} \right)^{1/3} \quad (3.7)$$

where the sum is over all moduli (including the one that decays). When the modulus decays, the relativistic decay products will reheat the universe to a temperature,

$$3H^2 = \frac{4\Gamma_\psi^2}{3} = m_p^{-2} \left(\frac{\pi^2}{30} \right) g_*(T_r) T_r^4, \quad (3.8)$$

$$\longrightarrow T_r = \left(\frac{40}{\pi^2} \right)^{1/4} g_*^{-1/4}(T_r) \sqrt{\Gamma_\psi m_p}, \quad (3.9)$$

or

$$T_r = \left(\frac{40}{\pi^2} \right)^{1/4} g_*^{-1/4}(T_r) \left(\frac{D_\psi m_\psi^3}{m_p} \right)^{1/2}. \quad (3.10)$$

Instead, if more than one modulus contributes to the energy density before decay the reheat temperature becomes

$$T_r = \left(\frac{40}{\pi^2} \right)^{1/4} g_*^{-1/4}(T_r) \left(\frac{m_\psi Y_\psi}{\sum_i m_i Y_i} \right)^{1/4} \left(\frac{D_\psi m_\psi^3}{m_p} \right)^{1/2}, \quad (3.11)$$

⁴We will take $g_{*s} = g_*$, which is true if all particles track the photon temperature. This is a good approximation for most of the history of the universe (prior to decoupling) [56].

where the sum is over all moduli (including the one that decays) and we note that this could lead to a subdominant radiation density compared to that of the remaining moduli. The entropy production is characterized by (assuming that $\Delta \gg 1$)

$$\Delta = \left(\frac{S_r}{S_d} \right) = \frac{g_{*s}(T_r) a^3(t_r) T_r^3}{g_{*s}(T_d) a^3(t_d) T_d^3}, \quad (3.12)$$

where T_d and T_r are the decay and reheat temperatures, respectively. Making use of (3.10), (3.12), and (3.6) we find

$$\begin{aligned} \Delta &= \frac{2}{15} (250\pi^2)^{1/4} \left(\frac{g_{*s}(T_r)}{g_{*s}(T_d)} \right) \left(\frac{g_{*s}(T_d)}{g_{*s}^{3/4}(T_r)} \right) \frac{m_\psi Y_\psi}{(\Gamma_\phi m_p)^{1/2}}, \\ &= \frac{2}{15} (250\pi^2)^{1/4} g_{*s}^{1/4}(T_r) \left(\frac{m_p}{D_\psi m_\psi} \right)^{1/2} Y_\psi, \end{aligned} \quad (3.13)$$

For the case that more than one modulus dominates the energy density before ψ decays, we have instead

$$\Delta = \frac{2}{15} (250\pi^2)^{1/4} g_{*s}^{1/4}(T_r) \left(\frac{m_p}{D_\psi m_\psi} \right)^{1/2} \left[\frac{\sum_i m_i Y_i}{m_\psi Y_\psi} \right]^{1/4} Y_\psi, \quad (3.14)$$

where the sum runs over all moduli that contribute to the energy density (including the decaying modulus ψ).

3.1.1 Moduli decay and BBN

From (3.14), we see that the decay of moduli can produce a substantial amount of entropy. Therefore, if any moduli present do not decay before the onset of BBN the resulting entropy production when decay occurs could result in devastating phenomenological consequences. However, another possibility is provided if the late-time decay of the moduli reheat the universe to temperatures greater than a few MeV. Such reheating will then allow BBN to proceed as usual. Requiring that the modulus decay exceeds this temperature one finds from (3.10) that $m_\psi \gtrsim 10$ TeV.

4. Summary of Results for the G_2 -MSSM

In this section, we give a brief summary of the results obtained in [37–39] for the G_2 -MSSM. Readers interested in more details should consult the references above. M theory compactifications on singular G_2 manifolds are interesting in the sense that they give rise to $\mathcal{N} = 1$ supersymmetry in four dimensions with non-Abelian gauge groups and chiral fermions. The non-Abelian gauge fields are localized along three-dimensional submanifolds of the seven extra dimensions whereas chiral fermions are supported at points at which there is a conical singularity. In order to study phenomenology concretely one has to address the issues of moduli stabilization, supersymmetry breaking and generation of the Hierarchy between the Electroweak and Planck scales. These issues can be fairly successfully addressed within the above framework.

In [37–39], it was shown that all moduli can be stabilized generically in a large class of M theory compactifications by non-perturbative effects. This happens in the zero-flux sector, our primary interest, when these compactifications support (at least two) non-abelian asymptotically free gauge groups. Strong gauge dynamics in these non-abelian (hidden sector) gauge groups gives rise to the non-perturbative effects which generate a moduli potential. When at least one of the hidden sectors also contains charged matter, under certain assumptions defining the above framework, supersymmetry is spontaneously broken in a metastable de Sitter vacuum which is tuned to the observed value. In the minimal framework, the hidden sector, including its moduli and hidden sector

matter, is described by $\mathcal{N} = 1$ supergravity with the following Kähler potential K , superpotential W and gauge kinetic function f at the compactification scale ($\sim M_{\text{unif}}$):

$$\begin{aligned}
K/m_p^2 &= -3 \ln(4\pi^{1/3} V_7) + \bar{\phi}\phi, & V_7 &= \prod_{i=1}^N s_i^{a_i} \\
W &= m_p^3 \left(C_1 P \phi^{-(2/P)} e^{ib_1 f_1} + C_2 Q e^{ib_2 f_2} \right); & b_1 &= \frac{2\pi}{P}, b_2 = \frac{2\pi}{Q} \\
f_1 = f_2 &\equiv f_{\text{hid}} = \sum_{i=1}^N N_i z_i; & z_i &= t_i + i s_i.
\end{aligned} \tag{4.1}$$

Here $V_7 \equiv \frac{\text{Vol}(X)}{l_{11}^7}$ is the volume of the G_2 manifold X in units of the eleven-dimensional Planck length l_{11} , and is a homogenous function of the s_i of degree $7/3$. A simple and reasonable ansatz therefore is $V_7 = \prod_{i=1}^N s_i^{a_i}$ with a_i positive rational numbers subject to the constraint $\sum_{i=1}^N a_i = \frac{7}{3}$. $\phi \equiv \det(Q\tilde{Q})^{1/2} = (2Q\tilde{Q})^{1/2}$ is the effective meson field (for one pair of massless quarks) and P and Q are proportional to one loop beta function coefficients of the two gauge groups which are completely determined by the gauge group and matter representations. The normalization constants C_1 and C_2 are calculable, given a particular G_2 -manifold. $f_{1,2}$ are the (tree-level) gauge kinetic functions of the two hidden sectors which have been taken to be equal for simplicity, (which is the case when the corresponding two 3-cycles are in the same homology class). s_i are the N geometric moduli of the G_2 manifold while t_i are axionic⁵ scalars. The integers N_i are determined from the topology of the three-dimensional submanifold which supports the hidden sector gauge groups.

If volume of the submanifold supporting the hidden sector gauge theories ($V_{\tilde{Q}}$) is large, the potential can be minimized analytically order-by-order in a $1/V_{\tilde{Q}}$ expansion. Physically, this expansion can be understood as an expansion in terms of the small gauge coupling of the hidden sector $-(\alpha_0)_{\text{hid}}$, which is self-consistent since the hidden sectors are assumed to be asymptotically free. The solution corresponding to a metastable minimum with spontaneously broken supersymmetry is given by

$$s_i = \frac{a_i}{N_i} \frac{3}{14\pi} \frac{P_{\text{eff}} Q}{Q - P} + \mathcal{O}(P_{\text{eff}}^{-1}), \tag{4.2}$$

$$|\phi|^2 = 1 - \frac{2}{Q - P} + \sqrt{1 - \frac{2}{Q - P}} + \mathcal{O}(P_{\text{eff}}^{-1}), \tag{4.3}$$

where $P_{\text{eff}} \equiv P \ln(C_1/C_2)$. The natural values of P and Q are expected to lie between $\mathcal{O}(1)$ and $\mathcal{O}(10)$. It is easy to see that a large P_{eff} corresponds to small α for the hidden sector

$$(\alpha_0^{-1})_{\text{hid}} = \text{Im}(f_{\text{hid}}) \approx \frac{Q}{2\pi(Q - P)} P_{\text{eff}} \tag{4.4}$$

implying that the expansion is effectively in P_{eff}^{-1} . The ϕ dependence of the potential at the minimum is essentially

$$V_0 \sim m_{3/2}^2 M_P^2 \left[|\phi|^4 + \left(\frac{4}{Q - P} + \frac{14}{P_{\text{eff}}} - 3 \right) |\phi|^2 + \left(\frac{2}{Q - P} + \frac{7}{P_{\text{eff}}} \right) \right] \tag{4.5}$$

Therefore, the vacuum energy vanishes if the discriminant of the above expression vanishes, i.e. if

$$P_{\text{eff}} = \frac{28(Q - P)}{3(Q - P) - 8} \tag{4.6}$$

⁵These essentially decouple from the moduli stabilization analysis. Hence they will not be considered further.

The above condition is satisfied when the contribution from the F -term of the meson field (F_ϕ) to the scalar potential cancels that from the $-3m_{3/2}^2$ term. In this vacuum, the F -term of the moduli F_i are much smaller than F_ϕ . Since phenomenologically interesting compactifications only arise for $Q - P = 3$ which corresponds to $P_{\text{eff}} = 84$ from (4.6), we will restrict our analysis to this particular choice.

4.1 Moduli Masses

Since in this paper we are interested in the evolution of the moduli (and meson) fields, it is important to study their masses in the vacuum described above. The set of gauge-singlet scalar fields includes N geometric moduli s_i associated with G_2 manifold and a hidden sector meson field ϕ . Since these moduli and meson will mix in general, the physical moduli correspond to mass eigenstates. The mass matrix can be written as:

$$(m_X^2)_{ij} = \left((a_i a_j)^{1/2} K_1 + \delta_{ij} K_2 \right) m_{3/2}^2 \quad (4.7)$$

$$(m^2)_{i\phi} = (a_i)^{1/2} K_3 m_{3/2}^2 \quad (4.8)$$

$$(m^2)_{\phi\phi} = K_4 m_{3/2}^2 \quad (4.9)$$

where K_1 to K_4 are obtained in [38]:

$$K_1 = \frac{16}{9261} \left(\frac{Q}{Q-3} \right)^2 P_{\text{eff}}^4 \quad (4.10)$$

$$K_2 = \frac{22}{3} - \frac{8}{9\phi_0^2} - 2\phi_0^2 - \left(1 + \frac{2}{3\phi_0^2} \right) \frac{36}{P_{\text{eff}}} \quad (4.11)$$

$$K_3 = \sqrt{\frac{2}{3}} \left(\frac{16}{1323} \right) \left(\frac{Q}{Q-3} \right)^2 \frac{P_{\text{eff}}^3}{\phi_0} \quad (4.12)$$

$$K_4 = \frac{32}{567} \left(\frac{Q}{Q-3} \right)^4 \frac{P_{\text{eff}}^4}{\phi_0^2} \quad (4.13)$$

where $\phi_0^2 \approx 0.734$. The special structure of the mass matrix allows us to find the eigenstates analytically. There is one heavy eigenstate with mass $m_{X_N} = (7K_1/3 + K_2)^{1/2} m_{3/2}$, $(N-1)$ degenerate light eigenstates with mass $m_{X_j} = (K_2)^{1/2} m_{3/2}$ and an eigenstate with mass $m_\phi = (K_4 - \frac{K_3^2}{K_1})^{1/2} m_{3/2}$. These mass eigenstates of the moduli fields are given by:

$$\begin{aligned} X_j &= \sqrt{\frac{a_{j+1}}{(\sum_{k=1}^j a_k)(\sum_{k=1}^{j+1} a_k)}} \left(\sum_{k=1}^j \sqrt{a_k} \delta s'_k - \frac{\sum_{k=1}^j a_k}{\sqrt{a_{j+1}}} \delta s'_{j+1} \right); \quad j = 1, 2, \dots, N-1 \\ X_N &= \sqrt{\frac{3}{7}} \sum_{k=1}^N \sqrt{a_k} \delta s'_k \end{aligned} \quad (4.14)$$

where $\delta s'_j = \sqrt{\frac{3a_j}{2s_j^2}} \delta s_j$ are the canonically normalized moduli fields. The normalized moduli fields can be related to the eigenstates by $\delta s'_i = U_{ij} X_j$, in which U_{ij} can be constructed using the eigenstates listed above. It is easy to show that $(\vec{X}_j)_i = U_{ij}$ for the eigenvector \vec{X}_j . In addition, there is another eigenstate X_ϕ corresponding to the meson field. Actually, the heavy eigenstate X_N and X_ϕ mix with each other. This mixing hardly changes the components of the eigenstate X_N and X_ϕ since $m_{X_N} \gg m_\phi$. However, the mass of the eigenstate X_ϕ is affected by the mixing. The masses m_{X_N} and m_ϕ only have a mild dependence on Q (for $P_{\text{eff}} = 84, Q - P = 3$), and do not depend on the number of moduli N at all. The mass of the light moduli m_{X_j} does not even depend on Q . Taking the expression for K_2 , one immediately finds that $m_{X_j} \approx 1.96 m_{3/2}$, $j = 1, \dots, N-1$. This

result is very important since light moduli are then not allowed to decay into gravitinos, essentially eliminating the moduli induced gravitino problem. Choosing a reasonable value of Q to be of $\mathcal{O}(10)$, one finds that m_ϕ is roughly around $2 m_{3/2}$ while m_{X_N} is roughly around $600 m_{3/2}$. Changing values of Q by $\mathcal{O}(1)$ hardly changes the moduli masses m_{X_N} and m_ϕ . Therefore, the above typical values will be used henceforth in our analysis. To summarize, the meson and moduli masses in the G_2 -MSSM can be robustly determined in terms of $m_{3/2}$.

4.2 Couplings and Decay Widths

Understanding the evolution of the moduli also requires a knowledge of the couplings of the moduli (meson) fields to the visible sector gauge and matter fields. Since all the moduli are stabilized explicitly in terms of the microscopic constants of the framework, all couplings of the moduli and meson fields to the MSSM matter and gauge fields can in principle be explicitly computed. Here we focus on the moduli couplings to MSSM matter and gauge fields. A different visible sector, as might arise from an explicit construction, will give rise to different couplings of the moduli fields in general, although with roughly the same moduli masses.

Here we will give a brief account of the important couplings of the moduli meson to visible gauge and matter fields and set the notation. Details are provided in Appendix B. The most important couplings of the moduli and meson fields involve two-body decays of the moduli and meson to gauge bosons, gauginos, squarks and slepton, quarks and leptons, higgses and higgsinos. The three-body decays are significantly more suppressed and will not be considered.

Let us start with the decay to gauge bosons and gauginos. The relevant part of the Lagrangian is given by:

$$\begin{aligned} \mathcal{L}_{\text{gauge boson, gaugino}} = & g_{X_k gg} X_k \hat{F}_{\mu\nu}^a \hat{F}^{a,\mu\nu} + g_{X_k \hat{g}\hat{g}} X_k \hat{\lambda}^a \hat{\lambda}^a + \\ & g_{\delta\hat{\phi}_0 \hat{g}\hat{g}} \delta\hat{\phi}_0 \hat{\lambda}^a \hat{\lambda}^a; \quad k = 1 \cdots N; \quad a = 1, 2, 3 \end{aligned} \quad (4.15)$$

Here, X_k , $\delta\hat{\phi}_0$, $\hat{F}_{\mu\nu}^a$ and $\hat{\lambda}^a$ are the normalized moduli, meson, gauge field strength and gaugino fields respectively. The expression for the couplings will be provided in Appendix B. It is important to note that the meson field does not couple to gauge bosons since the gauge kinetic function f_{sm} does not depend on ϕ_0 . The normalized moduli eigenstates X_k have already been discussed. The others can be written as:

$$\delta\hat{\phi}_0 = \frac{\delta\phi_0}{\sqrt{2}}; \quad \hat{F}_{\mu\nu}^a = \frac{F_{\mu\nu}^a}{\sqrt{\langle \text{Im}(f_{sm}) \rangle}}; \quad \hat{\lambda}^a = \frac{\lambda^a}{\sqrt{\langle \text{Im}(f_{sm}) \rangle}} \quad (4.16)$$

where f_{sm} is the gauge kinetic function for the visible SM gauge group. In the rest of the paper, we will neglect the hats for these normalized fields and m_p in the couplings for convenience.

The coupling of the moduli and meson fields to the MSSM non-higgs scalars (ie sfermions) turn out to be important, as will be seen later. Since the Standard model fermion masses (including that of the top) are much smaller than that of the moduli, the decay of the moduli and meson to these fermions will not be considered. The coupling to the MSSM sfermions can be written as:

$$\begin{aligned} \mathcal{L}_{\text{non-higgs scalars}} = & (g'_{X \tilde{f}\tilde{f}})_{i,\alpha\beta} \left[\partial_\mu (X_i \tilde{f}^{\alpha*}) \partial^\mu \tilde{f}_\alpha \right] - g_{X \tilde{f}\tilde{f}}^\alpha X_i \tilde{f}^{*\bar{\alpha}} \tilde{f}^\alpha \\ & + (g'_{\delta\hat{\phi}_0 \tilde{f}\tilde{f}})_{i,\alpha\beta} \left[\partial_\mu (\delta\hat{\phi}_0 \tilde{f}^{\alpha*}) \partial^\mu \tilde{f}_\alpha \right] - g_{\delta\hat{\phi}_0 \tilde{f}\tilde{f}}^\alpha \delta\hat{\phi}_0 \tilde{f}^{*\bar{\alpha}} \tilde{f}^\alpha \end{aligned} \quad (4.17)$$

where \tilde{f}_α are the canonically normalized scalar components of the visible chiral fields C_α , i.e. $\tilde{f}_\alpha = \frac{C_\alpha}{\sqrt{K_\alpha}}$. The couplings to the higgs and higgsinos are different due to the presence of the higgs bilinear $Z H_u H_d + h.c$ in the Kähler potential [39], which gives rise to contributions to the μ and

$B\mu$ parameters. In addition to the couplings similar as those in Eq.(B.17), there are additional couplings for scalar higgses, which can be schematically written as:

$$\begin{aligned} \mathcal{L}_{\text{higgs}} \supset & g_{X H_d H_u} X_j H_d H_u + g'_{X H_d H_u} \partial_\mu X_j \partial^\mu (H_d H_u) + c.c \\ & + g_{\delta\phi_0 H_d H_u} \delta\phi_0 H_d H_u + g'_{\delta\phi_0 H_d H_u} \partial_\mu \delta\phi_0 \partial^\mu (H_d H_u) + c.c \end{aligned} \quad (4.18)$$

As explained in [39], all higgs scalars except the SM-like higgs and all higgsinos are heavier than the gravitino, implying that the moduli and meson fields can only decay in this sector to the light SM-like higgs (h). The coupling to the SM-like higgs can be determined from the above coupling as explained in appendix B.

Finally, the moduli and meson fields can also decay directly to the gravitino. In fact, it turns out that the (non-thermal) production of gravitinos from direct decays dominates the thermal production of gravitinos in the early plasma. Therefore, it is important to consider the moduli and meson couplings to the gravitinos. Since the meson and light moduli are lighter than twice the gravitino mass (as seen from the previous subsection), only the heavy modulus can decay to the gravitino.

The explicit form of these couplings in terms of the microscopic constants is provided in appendix B. An important point to note is that these couplings are computed from the theory at a high scale, presumably the unification scale. However, since the temperature at which the moduli decay is much smaller than the unification scale, one has to RG evolve these couplings to scales at which these moduli decay (around their masses). The RG evolution has also been discussed in appendix B for the important couplings. Once the effective couplings of these moduli and meson are determined, one can compute the decay widths, as shown below.

For the G_2 -MSSM model, we have found that light moduli and meson dominantly decay to light higgses and squarks, while the heavy modulus dominantly decay to light higgses only. In appendix B, we have explicitly calculated the decay widths of the moduli X_k and meson. The widths of moduli can be schematically written as:

$$\begin{aligned} \Gamma_{X_k}^{\text{total}} &\equiv \frac{D_{X_k} m_{X_k}^3}{m_p^2} \approx \Gamma_{X_k \rightarrow gg} + \Gamma_{X_k \rightarrow \tilde{g}\tilde{g}} + \Gamma_{X_k \rightarrow \tilde{q}\tilde{q}} + \Gamma_{X_k \rightarrow hh} \\ &= \frac{7}{72\pi} \left(N_G (\mathcal{A}_1^{X_k} + \mathcal{A}_2^{X_k}) + \mathcal{A}_3^{X_k} + \mathcal{A}_4^{X_k} \right) \left(\frac{m_{X_k}^3}{m_p^2} \right), \end{aligned} \quad (4.19)$$

where $k = 1 \cdots N$ and $N_G = 12$ is the number of gauge bosons or gauginos. Note that $\mathcal{A}_3^{X_k}$ is significant only for $k = 1, 2, \dots, N-1$ (see appendix B). For the meson, the width can be written as:

$$\begin{aligned} \Gamma_{\delta\phi_0}^{\text{total}} &\equiv \frac{D_\phi m_\phi^3}{m_p^2} \approx \Gamma_{\delta\phi_0 \rightarrow \tilde{g}\tilde{g}} + \Gamma_{\delta\phi_0 \rightarrow \tilde{q}\tilde{q}} + \Gamma_{\delta\phi_0 \rightarrow hh} \\ &= \frac{7}{72\pi} (N_G \mathcal{A}_1^{\phi_0} + \mathcal{A}_2^{\phi_0} + \mathcal{A}_3^{\phi_0}) \left(\frac{m_\phi^3}{m_p^2} \right). \end{aligned} \quad (4.20)$$

4.3 Nature of the LSP

Before moving on to discuss the evolution of moduli in the G_2 -MSSM, it is important to comment on the nature of LSP in this framework. As explained in detail in [39], the G_2 -MSSM framework gives rise to Wino LSPs for choices of microscopic constants consistent with precision gauge unification. Therefore, in our analysis we focus on the Wino LSP case. As we will see, a Wino LSP turns out to be crucial in obtaining our final result.

5. Evolution of Moduli in the G_2 -MSSM

In this section, we apply the general discussion in Section 2 to the model of the G_2 -MSSM reviewed in the previous section. For clarity we will summarize our main results focusing on the more salient aspects of the physics, leaving the more technical details of the calculations to Appendix A. We will illustrate our computations with benchmark values, in order to get concrete numerical results, and comment on the choice of the benchmark values in section 7.

As discussed in Section 2, we assume that cosmological inflation and (p)reheating have provided adequate initial conditions for the post-inflationary universe.

5.1 Moduli Oscillations

As reviewed in the last section, we have a heavy modulus X_N , $N - 1$ light moduli X_i , and the scalar meson ϕ . These will begin to oscillate in the radiation dominated universe once the temperature cools and the expansion rate becomes comparable to their masses.

For a benchmark gravitino mass value⁶ of 50 TeV, the heavy modulus will begin oscillations first, at around $t_{X_N}^{osc} \approx 10^{-32}$ seconds, corresponding to a temperature of roughly $T = 10^{12}$ GeV. Following the heavy modulus, the other moduli will begin coherent oscillations around 10^{-30} s corresponding to a temperature of roughly 10^{11} GeV. These results are summarized in Table 1 below.

Modulus	Mass ($m_{3/2} = 50$ TeV)	Oscillation Time (seconds)
X_N	$m_{X_N} = 600 m_{3/2}$	$t_{osc}^{X_N} = 2 \times 10^{-32}$
X_ϕ	$m_\phi \lesssim 2 m_{3/2}$	$t_{osc}^\phi = 7 \times 10^{-30}$
X_i	$m_{X_i} \lesssim 2 m_{3/2}$	$t_{osc}^{X_i} = 7 \times 10^{-30}$

Table 1: Oscillation times for the G_2 -MSSM moduli

Since coherently oscillating moduli (ρ_m) scale relative to radiation as $\rho_m/\rho_r \sim a(t) \sim 1/T$, the moduli will quickly come to dominate the energy density of the universe, which is then matter dominated. Following the beginning of coherent oscillations of the heavy modulus, until the decay of all the moduli the universe will remain matter dominated. We will see that this, along with the entropy produced during moduli decays, results in negligible primordial thermal abundances of (s)particles compared with the non-thermal abundances coming from direct decays of the moduli. This will be crucial in addressing the gravitino problem and establishing a Wino-like LSP as a viable dark matter candidate through its non-thermal production.

5.2 Moduli Decays and Gravitino Production

As the universe continues to cool the expansion rate will eventually decrease enough so that the moduli are able to decay. This occurs when $H \sim \Gamma_X$, at which time the moduli will decay reheating the universe and producing substantial entropy. We will parameterize the decay rates of the G_2 -MSSM moduli as:

$$\Gamma_X = D_X \frac{m_X^3}{m_p^2}, \quad (5.1)$$

where Γ_X is the decay width for particle X . The decay times will be computed for a set of benchmark values of D_X for the various moduli (meson) which can be obtained by choosing particular (reasonable) sets of values of the microscopic constants (see appendix B for details).

⁶We give detailed numerical values for $m_{3/2} = 50$ TeV. It will be clear that values a factor of two or so smaller or larger than this will not change any conclusions in this and related analyses.

Modulus	Decay constant	Decay Time (seconds)
X_N	$D_{X_N} = 2$	$\tau_{X_N} = 9 \times 10^{-11}$
X_ϕ	$D_\phi = 710$	$\tau_\phi = 6 \times 10^{-6}$
X_i	$D_{X_i} = 4.00$	$\tau_{X_i} = 10 \times 10^{-4}$

Table 2: Decay constants and lifetimes for the G_2 -MSSM moduli for a set of benchmark microscopic values

5.2.1 Heavy Modulus Decay and Initial Thermal Abundances

Given the G_2 -MSSM values in Table 2 above, the heavy modulus will be the first to decay at around $10^{-11}s$. This decay will produce a large amount of entropy $\Delta_{X_N} = S_{after}/S_{before} \approx 10^{10}$ (even though the energy density of the heavy modulus is less than that of the meson and moduli), reheating the universe to a temperature $T_r^{X_N} = 41$ GeV. The entropy production will not only dilute the thermal abundances of all (s)particles, but also all the other moduli. One particularly important non-relativistic decay product of the heavy modulus is the gravitino. Gravitinos will be non-thermally produced by the modulus decay with a branching ratio $B_{3/2}^{X_N} = 0.07\%$, which yields a comoving abundance $Y_{3/2}^{(X_N)} = n_{3/2}/s \approx 10^{-9}$. This can be compared to the thermal abundance of gravitinos, which before modulus decay is $Y_{3/2}^{thermal} = 2.67 \times 10^{-8}$. This is further diluted by entropy production resulting from the decay, i.e. $Y_{3/2}^{thermal} \rightarrow Y_{3/2}^{thermal}/\Delta_{X_N} \approx 10^{-18}$. We see that the thermal contribution to the gravitino abundance is negligible compared to that from non-thermal production. A similar result follows for all other (s)particles that are thermally populated following inflation. Therefore, the primary source of (s)particles, and in particular gravitinos and Lightest SUSY Particles (LSPs), will result from non-thermal production resulting from decays of the moduli.

5.2.2 Meson/Light Moduli Decays and the Gravitino Problem

The decay of the heavy modulus is followed by the decay of the meson, at around $10^{-6}s$ (for benchmark values). The meson will decay before the light moduli because of a larger decay width compared to that for the light moduli (see appendix B for details). Similar to the heavy modulus, the meson contribution to the energy density is small compared to that of the $N - 1$ light moduli. Nevertheless, it produces some entropy ($\Delta_\phi \approx 121$) and reheats the universe to a temperature of around 134 MeV. The entropy production will again dilute the abundance of light moduli, and any (s)particles present, including the gravitinos from the heavy modulus decay.

The decay of the meson to gravitinos is particularly important, as this can result in the well-known gravitino problem. If the scalar decay yields a large number of gravitinos, these gravitinos can later decay producing a substantial amount of entropy that could spoil the successes of BBN.

The entropy produced from the decay of the meson and the other light moduli further dilutes the gravitino abundance from the heavy modulus. The primary contribution to the gravitino relic abundance comes from the decay of the heavy modulus since the other fields have masses of order $2 m_{3/2}$. After the decay of the meson, the energy density of the $N - 1$ light moduli is the dominant contribution to the total energy density of the Universe.

Given that the $N - 1$ light moduli are approximately degenerate in mass, their decays will occur at nearly the same time, after the decay of the meson. The resulting reheat temperature is found to be approximately 32 MeV, which is an acceptable temperature for consistency with the bound of 1 MeV set by BBN [57–60].

We note that the moduli decay rates have a strong dependence on the gravitino mass (as it sets the moduli mass scale). So, the decay of the light moduli being able to avoid BBN constraints is a result of the fact that the gravitino mass is relatively large ($m_{3/2} \gtrsim 50$ TeV). However, as explained

in detail in [39], the gauginos are significantly suppressed relative to the gravitinos allowing us to still obtain a light ($< \text{TeV}$) spectrum which can be seen at the LHC. The decay of each modulus will contribute to the total entropy production, and one finds that the total entropy production for the set of benchmark values of the microscopic constants is given by $\Delta_{X_i} = 418$. We also note that the light moduli lifetime depends inversely on the decay constant D_{X_i} , so if instead of taking relatively large values $D_{X_i} = 4$ we take relatively small values $D_{X_i} = 0.4$, we find a reheat temperature of 10 MeV which is still compatible with BBN⁷. The decay of light moduli to gravitinos is kinematically suppressed for the same reason as for the meson. The final gravitino abundance is then just the contribution from the heavy modulus decay diluted by the decay of the meson and light moduli and is $Y_{3/2}^{final} = Y_{3/2}^\phi / \Delta_{X_i} \approx 10^{-14}$. The above gravitino abundance is well within the upper bound on the gravitino abundance set by BBN constraints, as it will not lead to any significant entropy production at the time the gravitinos decay. Thus, we find that there is *no gravitino problem* in the G_2 -MSSM. In addition to the relativistic decay products, the light moduli will also decay appreciably into neutralinos (LSPs), which we consider in detail in the next section.

6. Dark Matter from the G_2 -MSSM

Natural models of electroweak symmetry breaking (EWSB) require additional symmetries and particles beyond those of the Standard Model. The additional particles typically come charged under additional discrete symmetries suppressing their decay to Standard Model particles (e.g. R-parity, KK-parity, etc.), so such models predict an additional, stable, weakly interacting particle with an electroweak scale mass, i.e. they naturally predict a candidate for Weakly Interacting Massive Particle (WIMP) cold dark matter. In the case of the G_2 -MSSM, this gives rise to a Wino-like neutralino which is the lightest supersymmetric particle (LSP) of the theory.

For completeness in section 6.1 we will review the standard calculation for computing the (thermal) dark matter relic density today. In section 6.2, we will then revisit this calculation for non-thermal production of LSPs resulting from scalar decay. In Section 6.3, we examine how non-thermal production is naturally realized in the G_2 -MSSM and predicts the Wino LSP as a viable WIMP candidate.

6.1 Standard Thermal Dark Matter

In the standard calculation of the relic abundance of LSPs it is assumed that prior to BBN the universe is radiation dominated. In particular, it is assumed that the dark matter particles are created from a thermal bath of radiation created from (p)reheating after inflation. In this radiation dominated universe, the Friedmann equation reads $3H^2 = m_p^{-2} \rho_r$, with $\rho_r = (\pi^2/30)g_*T^4$ the radiation density and g_* the number of relativistic degrees of freedom at temperature T .

The evolution of LSPs are given by the Boltzmann equation

$$\dot{n}_X = -3Hn_X - \langle \sigma v \rangle [n_X^2 - n_{eq}^2], \quad (6.1)$$

where $\langle \sigma v \rangle$ is the thermally averaged cross-section, n_X is the number density, and n_{eq} is the number density of the species in chemical equilibrium, i.e. $XX \leftrightarrow \gamma\gamma$, where γ is a relativistic particle such as the photon.

Assuming that initially the dark matter particles are relativistic ($m_X < T$) and in chemical equilibrium, then they will pass through three phases as the universe expands and cools. Initially their density will be determined by all the factors on the right side of (6.1). As long as the interactions of the particles take place on smaller time scales than the cosmic expansion then the particles will remain close to their equilibrium distributions. While the species is relativistic ($m_X <$

⁷See appendix A for a discussion of the range of the coefficients D_{X_i} .

T) this means that their comoving abundance is given by $Y_X = n_X/s \approx Y_X^{eq} = \text{const.}$. Once the universe cools enough from the cosmological expansion so that X becomes non-relativistic ($T < m_X$) then particle creation becomes more difficult (Boltzmann suppressed) and the comoving abundance tracks that of a non-relativistic species $Y_X \approx Y_X^{eq} = 0.145 x^{3/2} \exp(-x)$ where $x \equiv m_X/T$. The particle density will continue to decrease until the number of particles becomes so scarce that the expansion rate exceeds the annihilation rate and the particle species undergoes ‘freeze-out’. From (6.1) we see that at this time the number density is given by:

$$n_X = \frac{3H}{\langle\sigma v\rangle} \Big|_{T_f}, \quad (6.2)$$

where T_f indicates that this relation only holds at the time of freeze-out. Using (6.2) and $Y_X \approx Y_X^{eq}$ at the time of freeze-out, we find that freeze-out is only logarithmically sensitive to the parameters of the model, $x_f \equiv \frac{m_X}{T_f} \approx \ln [m_X m_p \langle\sigma v\rangle]$ and corrections are $\mathcal{O}(\ln \ln x_f)$. Taking both the cross-section and mass m_X to be weak scale at around 100 GeV we find that $x_f = 4$ and thus the freeze-out temperature is $T_f = m_X/25 \approx 4$ GeV. From (6.2) and (3.5), we find the comoving density at freeze-out:

$$Y_f = \frac{3H}{s\langle\sigma v\rangle}, \quad (6.3)$$

$$= \frac{45}{2\pi\sqrt{10}} \frac{1}{\sigma_0 g_*^{1/2}} \left(\frac{1}{m_p \langle\sigma v\rangle T_f} \right), \quad (6.4)$$

$$= \frac{45}{2\pi\sqrt{10}} \frac{1}{\sigma_0 g_*^{1/2}} \left(\frac{m_X}{m_p} \right) x_f, \quad (6.5)$$

where we have taken $\langle\sigma v\rangle = \sigma_0 m_X^{-2}$. We note that this answer is rather insensitive to the details of freeze-out, and the abundance is determined solely in terms of the properties of the produced dark matter (mass and cross-section). In particular, there is no dependence on the underlying microscopic physics of the theory.

6.2 Non-thermal Production from Scalar Decay

We know from the successes of BBN that at the time the primordial light elements were formed the universe was radiation dominated at a temperature greater than around an MeV. However, perhaps surprisingly, there is no evidence for a radiation dominated universe prior to BBN. In particular, we have seen that in the presence of additional symmetries and flat directions, scalar moduli can easily dominate the energy density of the universe and then later decay. The presence of these decaying scalars can alter the standard cold dark matter picture of the last section in significant ways.

To understand this, consider the decay of an oscillating scalar condensate ϕ , which decays at a rate $\Gamma_\phi \sim m_\phi^3/m_p^2$. When the expansion rate becomes of order the scalar decay rate ($H \sim \Gamma$) the scalars will decay into LSPs along with relativistic (s)particles which reheat the universe to a temperature T_r . If this reheat temperature is below that of the thermal freeze-out temperature of the particles $T_f \sim m_X/25$ then the LSPs will never reach chemical equilibrium. As an example, if we consider a scalar mass $m_\phi \sim 10 - 100$ TeV this gives rise to a reheat temperature $T_r \sim \sqrt{\Gamma_\phi m_p} \gtrsim$ MeV where $\Gamma_\phi \sim m_\phi^3/m_p^2$. The decay of ϕ in a supersymmetric setup could lead to LSPs with weak-scale masses $m_X \sim 100$ GeV, which have a thermal freeze-out temperature $T_f \sim m_X/25 \sim$ few GeV. We see that in this case $T_r < T_f$ is quite natural and the particles are non-thermally produced at a temperature below standard thermal freeze-out. Thus, the particles will be unable to reach chemical equilibrium.

Depending on the yield of dark matter particles from scalar decay, there are two possible outcomes of the non-thermally produced particles.

6.2.1 Case one: LSP Yield Above the Fixed Point

If the production of LSPs coming from scalar decay is large enough, then some rapid annihilation is possible at the time of their production. Since the particles are produced at the time of reheating, we know from the Boltzmann equation (6.1) that the critical density for annihilations to take place is:

$$n_X^c = \frac{3H}{\langle\sigma v\rangle} \Big|_{T_r}, \quad (6.6)$$

which is *different* from the result (6.2) in that here the reheat temperature and not the thermal freeze-out is the important quantity. This is very important because $T_r \sim \sqrt{\Gamma_\phi m_p}$ depends on the microscopic parameters of the theory as the reheat temperature is set by the decay rate of the scalar. In the standard case, we saw that the freeze-out temperature, or more precisely, the parameter $x_f \equiv m_X/T_f$ was only logarithmically sensitive to the parameters of the dark matter and gave no information at all about the underlying theory from which the dark matter was produced (e.g. scalars from the underlying microscopic physics).

Given that the initial number density of particles exceeds the above bound ($n_X(0) > n_X^c$), the LSPs will quickly annihilate until they reach the density (6.6). Thus, the critical value n_X^c serves as a fixed point for the number density, since any production above this limit will always result in the same yield of particles given by n_X^c . From this one finds the comoving density [40]

$$Y_X = \frac{c_1}{g_*^{1/2}} \frac{1}{m_p \langle\sigma v\rangle T_r} = Y_X^{std} \left(\frac{T_f}{T_r} \right), \quad (6.7)$$

where $c_1 = 45/(2\pi\sqrt{10})$. We see that non-thermal production can yield a greater comoving density than standard thermal production by a factor (T_f/T_r) . For the example considered above, namely $m_\phi \sim 10 - 100$ TeV, $m_X \sim 100$ GeV, and $T_r \sim$ few MeV we find the comoving density is enhanced by a factor $\sim 10^2 - 10^3$. One interesting consequence of this is it allows room for larger annihilation cross-sections for the LSPs. For example, in standard thermal production a Wino-like LSP leads to too small a relic density since its annihilation cross section is only s-wave suppressed. In the case of the G_2 -MSSM, non-thermal production is a natural consequence of the microscopic physics and a Wino LSP will provide a perfectly suitable WIMP candidate.

6.2.2 Case two: LSP Yield Below the Fixed Point

The other possibility is that the decay of the scalar yields few enough LSPs ($n_X(0) < n_X^c$) so that annihilation does not occur. Then the comoving abundance is simply given by

$$Y_X = B_\phi \Delta_\phi^{-1} Y_\phi^{(0)} \sim \frac{B_\phi n_\phi^{(0)}}{T_r^3}, \quad (6.8)$$

where B_ϕ is the branching ration of scalars to LSPs and $Y_\phi^{(0)}$ is the initial abundance of scalars in the decaying condensate. We note that again this result depends on the underlying physics of the UV theory, since both the branching ratio and the reheat temperature are coming from the physics of the scalar.

6.3 Dark Matter in the G_2 -MSSM

As shown in [39], the LSP in the G_2 -MSSM is predominantly Wino-like. There are two significant sources of these LSPs in the G_2 -MSSM – direct production from decays of both the gravitino and the light moduli. As explained earlier, the thermal abundance of LSPs in the early plasma after inflation is vastly diluted by the entropy productions from the heavy modulus, meson and the light moduli. Therefore, the thermal abundance of LSPs is negligible. In addition, the LSPs produced

from decays of the heavy modulus and the meson field are also diluted by the entropy production from the light moduli and are negligible as well.

The light moduli may decay to LSPs directly, or via decay to superpartners. From Section 4 the branching ratio for this process to occur for a set of benchmark values of the microscopic parameters is $B_{LSP}^{X_i} \sim 25\%$ and the comoving abundance is then found to be:

$$Y_{LSP}^{(X_i)} = \Delta_{X_i}^{-1} B_{LSP}^{X_i} (N-1) Y_{X_i}^{(\phi)} = 1.19 \times 10^{-7}, \quad (6.9)$$

where $\Delta_{X_i} = 417.7 [(N)/100]^{3/4}$ is the entropy production from the decay of all the light moduli X_i . Here we have taken benchmark value for the number of light moduli to be 100. The corresponding number density at the time of reheating is

$$n_{LSP} = s(T_r^{X_i}) Y_{LSP}, \quad (6.10)$$

$$= 1.79 \times 10^{-11} \text{ GeV}^3 \quad (6.11)$$

As discussed in the last section, we must compare this number density of LSPs to that of the critical density for annihilations (6.6). At the time of reheating from the light moduli the Hubble parameter is given by

$$H(t_r) = \left(\frac{\pi^2 g_*}{90} \right)^{1/2} \frac{(T_r^{X_i})^2}{m_p} = 4.48 \times 10^{-22} \text{ GeV}. \quad (6.12)$$

The dominant (s-wave) annihilation cross section for the LSPs ($\tilde{W}^0 \tilde{W}^0 \rightarrow W^+ W^-$) is given by

$$\langle \sigma v \rangle = \sigma_0 m_{LSP}^{-2} = \frac{1}{m_{LSP}^2} \frac{g_2^4 (1-x_w)^{3/2}}{2\pi (2-x_w)^2} = 3.26 \times 10^{-7} \text{ GeV}^{-2}, \quad (6.13)$$

where $x_w = m_w^2/m_{LSP}^2$, $m_w = 80.4 \text{ GeV}$ is the W -boson mass, and $g_2 \approx 0.65$ is the gauge coupling constant of $SU(2)_L$ at temperatures $T_r \sim \text{MeV}$, and this defines σ_0 . It is crucial that the cross-section is s-wave so that there is *no* temperature dependence in $\langle \sigma v \rangle$. We will comment more on this in section 7. Using (6.6) we find the fixed point density for annihilations

$$n_{LSP}^c = 4.12 \times 10^{-15} \text{ GeV}^3. \quad (6.14)$$

We see that the produced density is greater than the fixed point value $n_{LSP}^{X_i} > n_{LSP}^c$ and annihilations will occur. This corresponds to the ‘‘LSP yield above the fixed point’’ case discussed above. Thus, the LSPs produced will quickly annihilate down toward the fixed point value in less than a Hubble time. The relic density of dark matter is then given by the fixed point value (6.14) and the critical density of LSPs today coming from decay of the light moduli is

$$\Omega_{LSP}^{X_i} = \frac{m_{LSP} Y_{LSP}^c}{\rho_c/s_0} = \frac{1}{\rho_c/s_0} \left(\frac{45}{2\pi\sqrt{10g_*}\sigma_0} \right) \left(\frac{m_{LSP}^3}{m_p T_r^{X_i}} \right) = 0.76 h^{-2} \quad (6.15)$$

where s_0 and ρ_c are the entropy density and critical density today, respectively, and we have used the experimental value $\rho_c/s_0 = 3.6 \times 10^{-9} h^2 \text{ GeV}$ with h parameterizing the Hubble parameter today with median value $h = 0.71$.

In addition to this contribution, there is also the contribution from the decay of non-thermal gravitinos produced from the heavy modulus which have a final abundance $Y_{3/2}^{final} \approx 10^{-14}$. The contribution from gravitinos to the critical density of dark matter is then

$$\Omega_{LSP}^{(3/2)} = \frac{m_{LSP} Y_{3/2}^{final} s_0}{\rho_c} = 0.0008 h^{-2}, \quad (6.16)$$

which is negligible compared with that coming from the light moduli.

Thus, the total critical density in dark matter coming from the LSPs of the G_2 -MSSM is :

$$\Omega_{LSP} h^2 \approx 0.27 \left(\frac{m_{LSP}}{100 \text{ GeV}} \right)^3 \left(\frac{10.75}{g_*(T_r)} \right)^{1/4} \left(\frac{3.26 \times 10^{-7} \text{ GeV}^{-2}}{\langle \sigma v \rangle} \right) \left(\frac{4}{D_{X_i}} \right)^{1/2} \left(\frac{2m_{3/2}}{m_{X_i}} \right)^{3/2} \left(\frac{100 \text{ TeV}}{m_{3/2}} \right)^{3/2}, \quad (6.17)$$

where we have included all the parametric dependence of the answer derived in Appendix B. This value should be compared to the experimental value $\Omega_{CDM} h^2 = 0.111 \pm 0.006$ [61]. For those used to $\langle \sigma v \rangle$ in other units, note that $1 \text{ GeV}^{-2} = 0.4 \times 10^{-27} \text{ cm}^2$.

This result is not presented in terms of central values – rather it is the best value we can obtain. The LSP mass can be larger than 100 GeV, but not smaller. The decay constant D_{X_i} can be order 4, but a scan of the microscopic parameter space suggests a somewhat smaller value for the only calculable example so far known (see appendix B.4). A better understanding of the string theory could give 4 or a larger value. Whereas $m_{3/2}$ is somewhat constrained to be at most about 100 TeV by the parameters of the framework, as explained in [39]. Therefore, this framework is rather constrained and predictive. We view the closeness of this result as a success, and as an indication that improving the underlying theory may improve the agreement with data.

7. Discussion of Results

We have seen in the previous sections that for natural values of microscopic parameters, there is no moduli and gravitino problem in realistic G_2 compactifications. In addition, within the G_2 -MSSM, the non-thermal production of Wino LSPs from the light moduli give rise to a relic density with the right order of magnitude (up to factors of a few). It is possible that with a more sophisticated understanding of the theory, one could obtain a result more consistent with the observational results. It is also worthwhile to understand these results from a physical point of view. The results obtained above depend surprisingly little on many of the details of the microscopic parameters. In particular, there is essentially no dependence of the final relic density on the total number of moduli (N), the masses (m_{X_N}, m_ϕ) and couplings (D_{X_N}, D_ϕ) of the heavy modulus and meson fields as well as the initial amplitudes of the moduli (f_{X_k}) and meson (f_ϕ) fields. This is good in a sense since our understanding of the underlying theory and many of the above microscopic parameters is incomplete. However, the result *does* depend crucially on certain qualitative (and also some quantitative) features of the underlying physics, as we discuss below. In general it is better if results depend on the microscopic theory, since then data can tell us about the underlying theory.

One very important feature which helps avoid the gravitino problem is that the meson and light moduli have masses which are of order (actually slightly below) two gravitino masses, as we saw explicitly in Section 4.1. This kinematically suppresses their decays to the gravitino. The gravitino abundance is thus dominated by decay of the heavy modulus which is further diluted by entropy production from the decays of the meson and light moduli. Therefore, a natural mechanism for solving the gravitino problem in a generic setup is that the modulus which decays last does not decay to the gravitino. The moduli problem can also be easily solved in frameworks where the gravitino mass is $\gtrsim 10 \text{ TeV}$, which is naturally satisfied in the G_2 framework.

Another qualitative feature of the G_2 framework is that there is a hierarchy in the time scales of decay of the various moduli (meson) fields. Since the mass of the heavy modulus is much larger (~ 300 times) than that of the other moduli (meson), it decays much earlier. Also, from our current understanding of the Kähler potential of the meson and moduli fields, one finds (see appendix B) that the meson decays before the light moduli due to a larger decay width. The precise computation of the decay width depends on the nature of the Kähler potential for the meson and moduli and the Kähler metric for matter fields, and one might argue that there are inherent uncertainties in our understanding of these quantities. However, the only qualitative feature relevant for cosmological

evolution is that the meson decays before the light moduli. As long as the light moduli decay last (which we have argued in the appendix to be the natural case from our current understanding of the Kähler potential), the result does not depend on any of the masses and couplings of the heavy modulus or the meson field. The final result depends only on the masses and couplings of the light moduli which decay last. The same qualitative feature could be present in other frameworks arising from other limits of string/ M theory.

Now that it is clear that it is the light moduli decaying at the end which affect the final relic density, it is important to understand their effect more closely. In any theory of (soft) supersymmetry breaking, the mass of the light moduli will be set by the gravitino mass scale. In the context of low energy supersymmetry, the gravitino mass will typically be in the range 1 – 100 TeV. Therefore, the light moduli will also be typically in the above range⁸. Since the reheat temperature of the moduli basically depends on the moduli masses (assuming the coefficient D_{X_i} is $\mathcal{O}(1)$), the light moduli will typically give rise to a reheat temperature $T_r^{X_i}$ of $\mathcal{O}(1 - 100)$ MeV, which is far smaller than the freezeout temperature of the LSPs ($T_f^{LSP} \sim \text{GeV}$) which could be produced from the light moduli. This is true for the G_2 framework and could be true for many other frameworks as well. Therefore, with $T_r^{X_i} < T_f^{LSP}$, the final outcome for the relic density will depend on the whether the number density of the LSPs produced from the light moduli ($n_{LSP}^{(X_i)}$) is greater or smaller than the critical number density at $T_r^{X_i}$ ($n_{LSP}^{(c)}|_{T_r^{X_i}}$).

For the G_2 framework, for natural values of the microscopic parameters one finds that $n_{LSP}^{(X_i)} > n_{LSP}^{(c)}|_{T_r^{X_i}}$ as shown in section 6.3. This is equivalent to the inequality:

$$B_{LSP}^{(X_i)} D_{X_i} > \frac{1.5}{\sigma_0} \left(\frac{m_{LSP}^2}{m_{X_i}^2} \right) \approx 120 \gamma^2$$

with $\gamma \equiv \frac{m_{LSP}}{m_{3/2}}$ (7.1)

where σ_0 is defined by (6.13) and we have used $m_{X_i} \approx 1.96 m_{3/2}$. As explained in [39], the quantity γ depends predominantly on δ , which characterizes the threshold correction to the gauge couplings at the unification scale. The dependence on other microscopic parameters such as V_7 and C_2 (see section 4) is largely absorbed into the gravitino mass. The suppression factor γ depends almost linearly on $|\delta|$, and typically takes value in the range $\sim (1 - 6) \times 10^{-3}$. Now, the constraint (7.1) is easy to understand. For natural values of microscopic parameters in the G_2 framework, one has $B_{LSP}^{(X_i)} = \mathcal{O}(25\%)$, $D_{X_i} = \mathcal{O}(1)$ (see appendix B) which easily satisfy (7.1) above. In order for other frameworks to realize this situation, a criterion similar to (7.1) needs to be satisfied.

When (7.1) is satisfied, the final relic density can be written as (see (6.14) and (6.17)):

$$\begin{aligned} \Omega_{LSP} h^2 &\approx \frac{m_{LSP} Y_{LSP}^c}{\rho_c/s_0} = \frac{1}{\rho_c/s_0} \left(\frac{45}{2\pi\sqrt{10g_*}\sigma_0} \right) \left(\frac{m_{LSP}^3}{m_p T_r^{X_i}} \right) \\ &\approx \frac{1}{\rho_c/s_0} \left(\frac{45}{2\sqrt{10\pi}(40g_*)^{1/4}\sigma_0} \right) \left(\frac{m_{LSP}^3}{D_{X_i}^{1/2} m_p^{1/2} m_{X_i}^{3/2}} \right) \\ &\approx 18 \text{ GeV}^{-3/2} \left(\frac{m_{LSP}^{3/2} \gamma^{3/2}}{D_{X_i}^{1/2}} \right) = 18 \text{ GeV}^{-3/2} \left(\frac{m_{3/2}^{3/2} \gamma^3}{D_{X_i}^{1/2}} \right) \end{aligned} \quad (7.2)$$

An upper bound on the observed value of the relic density implies that smaller values of γ and m_{LSP} and larger values of D_{X_i} are preferred. A small γ implies that for a given LSP mass a

⁸This is however not true for Large Volume compactifications as the lightest modulus in that case is much lighter than $m_{3/2}$ [25].

heavier gravitino is preferred implying that the moduli be correspondingly heavier. Also, since γ is roughly linear in $|\delta|$, smaller values of $|\delta|$ are preferred. These features can be seen easily from the plots in figures 1 and 2. Figure 1 shows a contour plot of the relic density in the $D_{X_i} - m_{3/2}$ plane for two (large and small) values of $|\delta|$ which correspond to two (large and small) values of γ . Figure 2 shows the dependence of the relic density on the reheat temperature of the light moduli

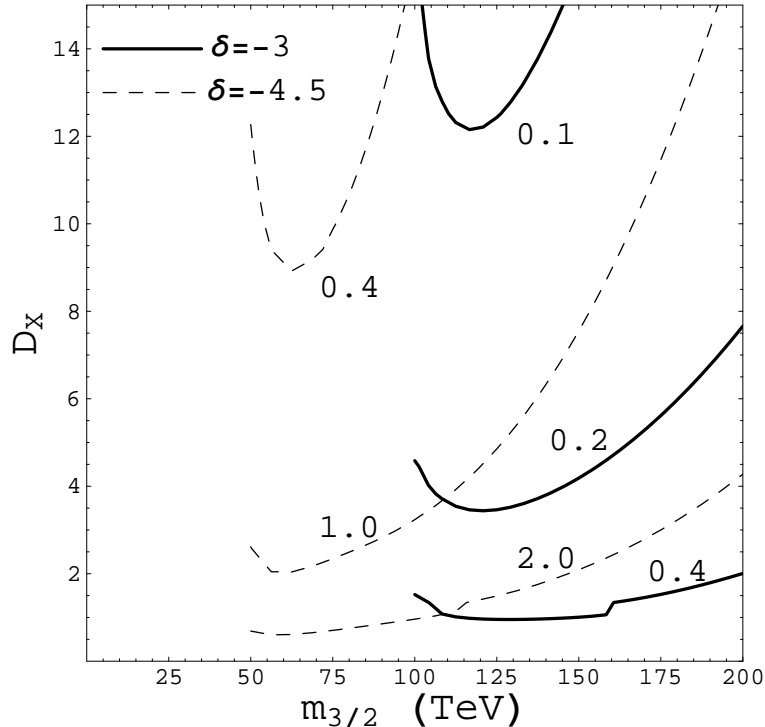


Figure 1: The contour plot of the relic density in the G_2 -MSSM in the $D_{X_i} - m_{3/2}$ plane for two (large and small) values of $|\delta|$ which correspond to two (large and small) values of γ . The solid lines are for $\delta = -3$ (a correction to α_{unif}^{-1} of order $3/26$), and the dashed lines for $\delta = -4.5$.

($T_r^{X_i}$). As seen from the first line in (7.2), the relic density is inversely proportional $T_r^{X_i}$ implying that a higher reheat temperature is preferred. A higher $T_r^{X_i}$ corresponds precisely to a larger D_{X_i} and m_{X_i} (larger $m_{3/2}$) as explained above.

As explained in section 6.3, the nature of the LSP is also crucial to the final result for the relic density. For the G_2 framework, the annihilation cross-section is s-wave and does not depend on $T_r^{X_i}$. On the other hand, if the LSP were Bino, the cross-section would be p-wave suppressed and would depend linearly on $T_r^{X_i}/m_{LSP}$, thereby making it suppressed relative to the s-wave result. This would make the relic density much larger than the result obtained for the s-wave case above. Therefore, the upper bound on relic density prefers small mixing angles (or vanishing mixing angles, as in the G_2 -MSSM) with the Bino and Higgsino components. This can be seen from figure 3.

8. Summary and Future Directions

In this paper we have emphasized the importance of the cosmological moduli and gravitino problems and the relation to adequate generation of dark matter in thermal equilibrium, or generation of too much dark matter non-thermally in string/ M theory frameworks. Focussing on G_2 compactifications, in particular on the G_2 -MSSM, we have found that the decay of moduli in this framework is rather naturally consistent with BBN constraints, and the associated large entropy production at

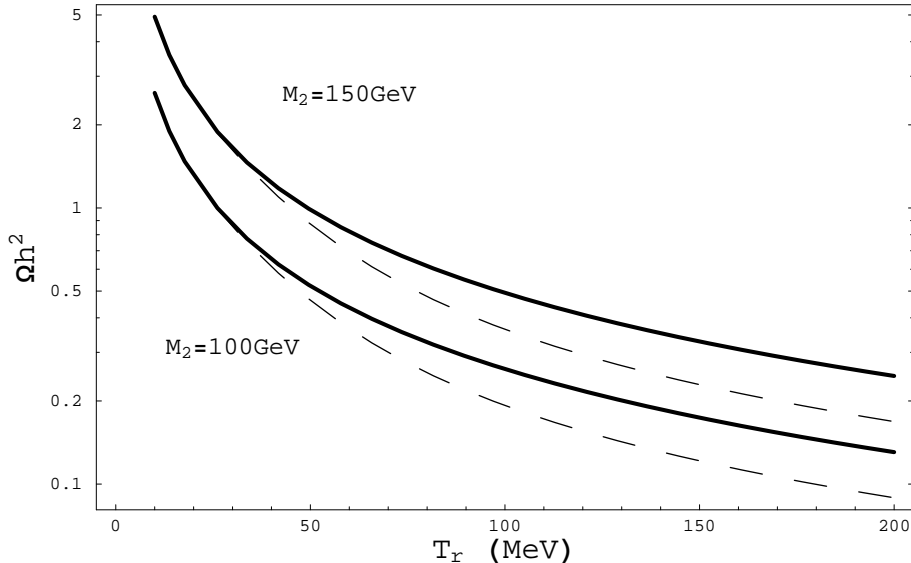


Figure 2: The LSP relic density for the G_2 -MSSM plotted as a function of the reheat temperature of the light moduli. The solid line assumes no coannihilation with charged Winos; the dashed line includes coannihilation with charged Winos.

late times (but before BBN) results in an avoidance of the gravitino problem(s). Moreover, we have seen that the late decay of the light moduli into Wino-like neutralinos leads to a nearly acceptable relic density of cold dark matter. This result arises from a combination of entropy production and LSPs from moduli decay giving an adequate relic density from non-thermal production of dark matter. This process offers an explicit example of how *thermal dark matter production is not the dominant source of cosmological dark matter, especially in the presence of moduli*. The LSP is Wino-like here as well as in anomaly mediated theories, but for interestingly different reasons – here the tree level gaugino masses are universal but about the same size as the anomaly mediated ones, and the finite one loop Higgsino is comparable with both.

The result for the final relic density depends parametrically on the couplings and mass of the light moduli (which decay last) and the mass of the LSP. The masses of the light moduli and the LSP are set by the gravitino mass scale and depend on a set of underlying microscopic parameters of the theory. The couplings of the moduli depend on the Kähler potential of the theory. Since our understanding of the Kähler potential is incomplete, it is only possible to make reasonable assumptions to proceed, which is what we have done, but one can see that most of the results are insensitive to these uncertainties. That is because the moduli decays produce a large number density of LSPs, which then annihilate down to the final relic density that only depends on the reheating temperature. From (7.2) and figure 1, we see that an upper bound on the relic density prefers a light LSP, heavy gravitino and large couplings to the visible sector parameterized by D_{X_i} (defined in (4.19)). These results obtained have been explained in terms of the underlying qualitative features of the framework. These qualitative features could be present in other string/ M theory frameworks as well, leading to similar results.

There is not yet a satisfactory inflation mechanism for the G_2 -MSSM. This is under study.

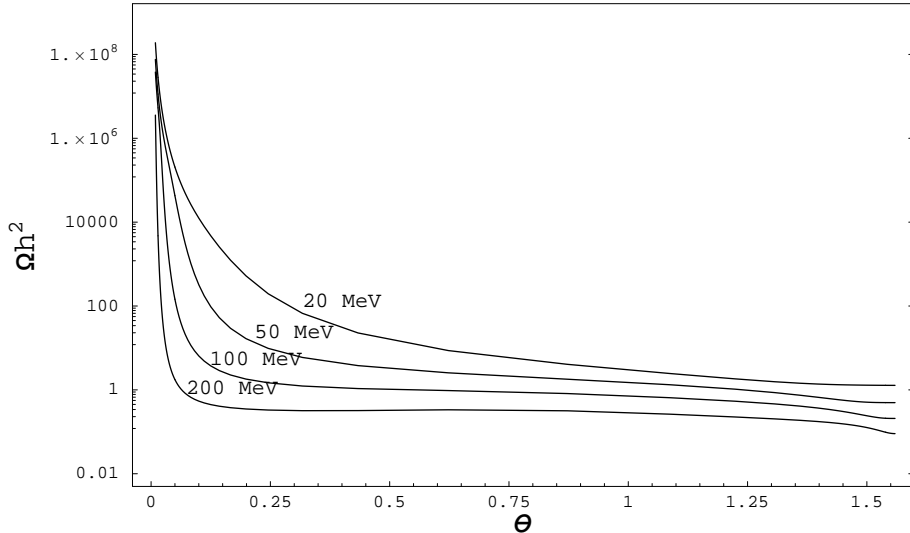


Figure 3: The LSP relic density in the G_2 -framework plotted as a function of the mixing angle of Bino and Wino for $M_2 = 100\text{GeV}$.

Fortunately, our results are not sensitive to that. We assume only that at an early time inflation ends and the energy density of the universe is dominated by moduli settling into the minimum of the potential.

In future, one would like to understand the origin of the baryon asymmetry in the Universe (BAU) within string/ M theory frameworks. In the G_2 framework, the large entropy production resulting from the decay of the moduli was crucial for addressing the gravitino problem. However, this entropy will also act to reduce any initial baryon asymmetry. Therefore, one requires a large initial asymmetry or a late-time mechanism for regeneration of the asymmetry. For example, a large initial baryon asymmetry could arise from the Affleck-Dine mechanism [62], or it could happen that the superpartner parameter space allows for late-time electroweak baryogenesis. This is work in progress.

Understanding the above issues would be crucial to solving the “cosmological inverse problem” (see [63,64] for some preliminary work in this direction), usually considered separate from the “LHC Inverse Problem” [65]. Within the context of realistic string/ M theory frameworks, however, the two inverse problems merge into one “inverse problem” as the microscopic parameters characterizing the underlying physics of any framework have predictions (at least in principle) for both particle physics as well as cosmological observables, thereby providing unique connected insights into these basic issues.

9. Acknowledgements

We thank Lotfi Boubekeur, Joe Conlon, Paolo Creminelli, Sera Cremonini, Alan Guth, Lawrence Hall, Nemanja Kaloper, Joern Kersten, Siew-Phang Ng, Piero Ullio, Filippo Vernizzi, and Lian-Tao Wang for useful discussions. The research of K.B., G.L.K., P.K., J.S. and S.W. is supported in part

by the US Department of Energy. S.W. would also like to thank the MIT Center for Theoretical Physics for hospitality. J.S. would also like to thank the Institute for Advanced Study - Princeton for hospitality.

A. Cosmology of the G_2 -MSSM Moduli – A detailed treatment

In this appendix, we include detailed calculations leading to the abundances, entropy production, and reheat temperatures quoted in the paper for sets of benchmark values of the microscopic parameters. The computation of couplings and decay widths of the moduli and meson fields in terms of the microscopic parameters which motivate the benchmark values will be given in appendix B. We have retained the parametric sensitivity to the gravitino mass, number of moduli (topology), and the overall couplings of the moduli (meson) in order to address the robustness and plausibility of the framework.

A.1 Heavy modulus oscillations

At the time the heavy moduli (X_N) starts coherent oscillations the universe is radiation dominated and the Hubble equation is given by

$$3H^2 = 3 \left(\frac{1}{2} m_{X_N} \right)^2 = m_p^{-2} \left(\frac{\pi^2}{30} \right) g_* T^4. \quad (\text{A.1})$$

The temperature at which the modulus starts oscillating is then given by

$$\begin{aligned} T_{osc}^{X_N} &= \left(\frac{90}{4\pi^2} \right)^{1/4} g_*^{-1/4} (T_{osc}^{X_N}), \\ &= 2.70 \times 10^{12} \left(\frac{228.75}{g_*(T_{osc}^{X_N})} \right)^{1/4} \left(\frac{m_{X_N}}{600 m_{3/2}} \right)^{1/2} \text{ GeV}. \end{aligned} \quad (\text{A.2})$$

From this we find the entropy density

$$s(T_{osc}^{X_N}) = \frac{2\pi^2}{45} g_{osc} T_{osc}^3, \quad (\text{A.3})$$

$$= 1.98 \times 10^{39} \left(\frac{g_{osc}}{228.75} \right)^{1/4} \left(\frac{m_{X_N}}{600 m_{3/2}} \right)^{3/2} \text{ GeV}^3, \quad (\text{A.4})$$

and the comoving abundance is then

$$\begin{aligned} Y_{X_N}^{(0)} &= \frac{1}{2} m_{X_N} f_{X_N}^2 s^{-1}(T_{osc}^{X_N}), \\ &= 4.51 \times 10^4 \left(\frac{228.75}{g_*(T_{osc})} \right)^{1/4} \left(\frac{f_{X_N}}{m_p} \right)^2 \left(\frac{600 m_{3/2}}{m_{X_N}} \right)^{1/2}, \end{aligned} \quad (\text{A.5})$$

The oscillating modulus will quickly come to dominate the radiation density and the temperature at this time is given by

$$T_{eq}^{X_N} = 1.80 \times 10^{12} \left(\frac{228.75}{g_*(T_{osc}^{X_N})} \right)^{1/4} \left(\frac{m_{X_N}}{600 m_{3/2}} \right)^{1/2} \left(\frac{f_{X_N}}{m_p} \right)^2 \text{ GeV}, \quad (\text{A.6})$$

so that we see once the modulus starts coherent oscillations it quickly overtakes the energy density (i.e., $T_{eq}^{X_N} \approx T_{osc}^{X_N}$).

A.2 Meson and Light Moduli Oscillations

Because the meson and light moduli are approximately degenerate in mass (i.e. $m_\phi = m_{X_i}$) they will begin to oscillate at the same time,

$$3H^2 = 3 \left(\frac{2}{3} m_\phi \right)^2 = m_p^{-2} \left(\frac{\pi^2}{30} g_*(T_{osc}^\phi) (T_{osc}^\phi)^4 + m_{X_N} Y_{X_N} s(T_{osc}^\phi) \right). \quad (\text{A.7})$$

Noting that the radiation term has already become negligible compared to the heavy modulus density we find the temperature at this time is given by

$$T_{osc}^\phi = \left(\frac{30}{\pi^2} \right)^{1/3} \left[\frac{m_\phi^2 m_p^2}{g_*(T_{osc}^\phi) m_{X_N} Y_{X_N}} \right]^{1/3}, \quad (\text{A.8})$$

$$= 8.24 \times 10^{10} \left(\frac{228.75}{g_*(T_{osc}^{X_N})} \right)^{1/4} \left(\frac{m_\phi}{2 m_{3/2}} \right)^{2/3} \left(\frac{600 m_{3/2}}{m_{X_N}} \right)^{1/6} \left(\frac{m_p}{f_{X_N}} \right)^{2/3} \text{ GeV} \quad (\text{A.9})$$

which is in excellent agreement with the exact answer obtained numerically (including radiation) $T_{osc}^\phi = 9.97 \times 10^{10}$. The entropy density at this time is

$$s(T_{osc}^\phi) = 5.62 \times 10^{34} \left(\frac{g_*(T_{osc}^{X_N})}{228.75} \right)^{1/4} \left(\frac{m_\phi}{2 m_{3/2}} \right)^2 \left(\frac{600 m_{3/2}}{m_{X_N}} \right)^{1/2} \left(\frac{m_p}{f_{X_N}} \right)^2 \text{ GeV}^3, \quad (\text{A.10})$$

The meson ϕ initial abundance is then

$$Y_\phi^{(0)} = 5.30 \times 10^6 \left(\frac{228.75}{g_*(T_{osc})} \right)^{1/4} \left(\frac{f_\phi}{m_p} \right)^2 \left(\frac{f_{X_N}}{m_p} \right)^2 \left(\frac{m_{X_N}}{600 m_{3/2}} \right)^{1/2} \left(\frac{2 m_{3/2}}{m_\phi} \right). \quad (\text{A.11})$$

The light moduli will begin coherent oscillations at roughly the same time as the meson. Their abundance is then given by

$$Y_{X_i}^{(0)} = (N-1) Y_\phi^{(0)} = 5.25 \times 10^8 \left(\frac{N-1}{99} \right) \left(\frac{228.75}{g_*(T_{osc})} \right)^{1/4} \left(\frac{f_{X_i}}{m_p} \right)^2 \left(\frac{f_{X_N}}{m_p} \right)^2 \left(\frac{m_{X_N}}{600 m_{3/2}} \right)^{1/2} \left(\frac{2 m_{3/2}}{m_{X_i}} \right), \quad (\text{A.12})$$

where we have implicitly assumed that because the masses of the meson and light moduli are approximately degenerate they will have equal oscillation amplitudes⁹.

A.3 Heavy Modulus Decay

Once the Hubble parameter decreases to the point when $H \approx \Gamma_{X_N}$, the heavy modulus decays and from (3.11) the corresponding reheat temperature is,

$$T_r^{X_N} = 41.40 \left(\frac{10.75}{g_*(T_r^{X_N})} \right)^{1/4} \left(\frac{D_{X_N}}{1.6} \right)^{1/2} \left(\frac{m_{X_N}}{600 m_{3/2}} \right)^{3/2} \left(\frac{m_p}{f_\phi} \right)^{1/2} \left(\frac{100}{N} \right)^{1/4} \text{ GeV}. \quad (\text{A.13})$$

To understand the N and ϕ dependence in this expression, we note that from (3.11) the reheat temperature includes the factor,

$$\left(\frac{m_{X_N} Y_{X_N} + m_\phi Y_\phi + m_{X_i} Y_{X_i}}{m_{X_N} Y_{X_N}} \right)^{1/4} \quad (\text{A.14})$$

Using that the meson and light moduli have degenerate mass and therefore equal oscillation amplitudes (i.e. $m_{X_i} Y_{X_i} = (N-1) m_\phi Y_\phi$) we find

$$\left(1 + N \frac{m_\phi Y_\phi}{m_{X_N} Y_{X_N}} \right)^{-1/4} \approx \left(N \frac{m_\phi Y_\phi}{m_{X_N} Y_{X_N}} \right)^{-1/4} \quad (\text{A.15})$$

⁹We note that initially this may not be the case, but at the onset of coherent oscillations (much less than a Hubble time) the system will settle into this symmetric configuration.

which leads to the parametric dependence in the reheat temperature.

Using (3.14) the entropy increase resulting from the heavy modulus decay is

$$\begin{aligned} \Delta_{X_N} &= 4.35 \times 10^{10} \left(\frac{g_*(T_r^{X_N})}{10.75} \right)^{1/4} \left(\frac{228.75}{g_*(T_{osc}^{X_N})} \right)^{1/4} \left(\frac{f_{X_N}}{m_p} \right)^2 \left(\frac{1.6}{D_{X_N}} \right)^{1/2} \\ &\quad \times \left(\frac{600 m_{3/2}}{m_{X_N}} \right) \left(\frac{f_\phi}{m_p} \right)^{1/2} \left(\frac{N}{100} \right)^{1/4}, \end{aligned} \quad (\text{A.16})$$

where we have again used (A.15). Therefore, after the decay the other moduli abundances are given by

$$\begin{aligned} Y_\phi^{(X_N)} &= \Delta_{X_N}^{-1} Y_\phi^{(0)}, \\ &= 1.22 \times 10^{-4} \left(\frac{10.75}{g_*(T_r^{X_N})} \right)^{1/4} \left(\frac{D_{X_N}}{1.6} \right)^{1/2} \left(\frac{f_\phi}{m_p} \right)^{3/2} \left(\frac{m_{X_N}}{600 m_{3/2}} \right)^{3/2} \left(\frac{2 m_{3/2}}{m_\phi} \right) \left(\frac{100}{N} \right)^{1/4} \end{aligned} \quad (\text{A.17})$$

$$\begin{aligned} Y_{X_i}^{(X_N)} &= \Delta_{X_N}^{-1} Y_{X_i}^{(0)}, \\ &= 1.21 \times 10^{-2} \left(\frac{10.75}{g_*(T_r^{X_N})} \right)^{1/4} \left(\frac{D_{X_N}}{1.6} \right)^{1/2} \left(\frac{f_{X_i}}{m_p} \right)^{3/2} \left(\frac{m_{X_N}}{600 m_{3/2}} \right)^{3/2} \left(\frac{2 m_{3/2}}{m_{X_i}} \right) \left(\frac{N}{100} \right)^{3/4}, \end{aligned} \quad (\text{A.18})$$

where we have again used $N - 1 \approx N$. There is also a decay to gravitinos with branching ratio $B_{3/2}^{(X_N)} = 0.2\% = 0.002$. The corresponding comoving abundance is thus,

$$\begin{aligned} Y_{3/2}^{(X_N)} &= 2 \times B_{3/2} \times \frac{Y_{X_N}^{(0)}}{\Delta_{X_N}}, \\ &= 1.45 \times 10^{-9} \left(\frac{B_{3/2}}{0.07\%} \right) \left(\frac{10.75}{g_*(T_r^{X_N})} \right)^{1/4} \left(\frac{D_{X_N}}{1.6} \right)^{1/2} \left(\frac{m_{X_N}}{600 m_{3/2}} \right)^{1/2} \left(\frac{m_p}{f_\phi} \right)^{1/4} \left(\frac{100}{N} \right)^{1/4}, \end{aligned} \quad (\text{A.19})$$

A.4 Meson Decay

When the meson decays, its contribution to the total energy density will be less than that of the other $N - 1$ light moduli. The universe will be matter dominated before and after the decay, but because the two energy sources are comparable there is a somewhat significant entropy production. The meson decay reheats the universe to a temperature

$$T_r^\phi = 134 \times \left(\frac{100}{N} \right)^{1/4} \left(\frac{10.75}{g_*(T_r)} \right)^{1/4} \left(\frac{D_\phi}{711.6} \right)^{1/2} \left(\frac{m_\phi}{2 m_{3/2}} \right)^{3/2} \text{ MeV}. \quad (\text{A.20})$$

The entropy increase is given by

$$\Delta_\phi = 121 \times \left(\frac{D_{X_N}}{1.6} \right)^{1/2} \left(\frac{711.6}{D_\phi} \right)^{1/2} \left(\frac{m_{X_N}}{600 m_{3/2}} \right)^{3/2} \left(\frac{2 m_{3/2}}{m_\phi} \right)^{3/4} \left(\frac{f_\phi}{m_p} \right)^{3/2}. \quad (\text{A.21})$$

The decay of the meson will further dilute the other moduli, we find

$$\begin{aligned} Y_{X_i}^{(\phi)} &= \Delta_{X_N}^{-1} \Delta_\phi^{-1} Y_{X_i}^{(0)}, \\ &= 9.94 \times 10^{-5} \left(\frac{N}{100} \right)^{3/4} \left(\frac{10.75}{g_*(T_r)} \right)^{1/4} \left(\frac{D_\phi}{711.6} \right)^{1/2} \left(\frac{2 m_{3/2}}{m_{X_i}} \right)^{1/4}. \end{aligned} \quad (\text{A.22})$$

The decay of both the meson and the light moduli to gravitinos is kinematically suppressed, so that the only source of gravitinos comes from the decay of the heavy modulus. This abundance after the decay of the meson is then

$$\begin{aligned} Y_{m_{3/2}}^{(\phi)} &= \Delta_\phi^{-1} Y_{m_{3/2}}^{(X_N)}, \\ &= 1.19 \times 10^{-11} \left(\frac{B_{3/2}^{(X_N)}}{0.07\%} \right) \left(\frac{100}{N} \right)^{1/4} \left(\frac{10.75}{g_*(T_r)} \right)^{1/4} \left(\frac{D_\phi}{711.6} \right)^{1/2} \left(\frac{m_\phi}{2 m_{3/2}} \right)^{3/4} \left(\frac{600 m_{3/2}}{m_{X_N}} \right) \left(\frac{m_p}{f_\phi} \right)^{7/4} \end{aligned} \quad (\text{A.23})$$

A.5 Light Moduli Decays

The decay of the light moduli results in a reheating temperature

$$T_r^{X_i} = 31.7 \times \left(\frac{10.75}{g_*(T_r)} \right)^{1/4} \left(\frac{m_{X_i}}{2 m_{3/2}} \right)^{3/2} \left(\frac{D_{X_i}}{4} \right)^{1/2} \text{ MeV}, \quad (\text{A.24})$$

which agrees with the bounds set by BBN (i.e. $T_r^{X_i} > 1 \text{ MeV}$). The resulting entropy production is

$$\Delta_{X_i} = 417.7 \times \left(\frac{D_\phi}{711.6} \right)^{1/2} \left(\frac{4}{D_{X_i}} \right)^{1/2} \left(\frac{2 m_{3/2}}{m_{X_i}} \right)^{3/4} \left(\frac{N}{100} \right)^{3/4}. \quad (\text{A.25})$$

The new gravitino abundance is given by

$$\begin{aligned} Y_{m_{3/2}}^{(X_i)} &= \Delta_{X_i}^{-1} Y_{m_{3/2}}^{(\phi)}, \quad (\text{A.26}) \\ &= 2.86 \times 10^{-14} \left(\frac{B_{3/2}^{(X_N)}}{0.07\%} \right) \left(\frac{100}{N} \right) \left(\frac{10.75}{g_*(T_r)} \right)^{1/4} \left(\frac{m_\phi}{2 m_{3/2}} \right)^{3/2} \left(\frac{600 m_{3/2}}{m_{X_N}} \right) \left(\frac{D_{X_i}}{4} \right)^{1/2} \left(\frac{m_p}{f_\phi} \right)^{7/4} \end{aligned} \quad (\text{A.27})$$

which is small enough to avoid the gravitino problem. The light moduli will decay into LSPs yielding an abundance

$$\begin{aligned} Y_{LSP}^{(X_i)} &= \Delta_{X_i}^{-1} B_{LSP}^{X_i} Y_{X_i}^{(\phi)}, \\ &= 1.19 \times 10^{-7} \left(\frac{B_{LSP}^{X_i}}{25\%} \right) \left(\frac{10.75}{g_*(T_r)} \right)^{1/4} \left(\frac{m_{X_i}}{2 m_{3/2}} \right)^{1/2} \left(\frac{D_{X_i}}{4} \right)^{1/2}, \end{aligned} \quad (\text{A.28})$$

where $B_{LSP}^{X_i}$ is the branching ratio for the decay of the light moduli to LSPs. This corresponds to a number density at the time of decay of $n_{LSP} = 1.79 \times 10^{-11} \text{ GeV}^3$.

As we noted in the text, this abundance is produced below the freeze-out temperature of the LSPs (non-thermal production) and is greater than the critical density (6.6) for annihilations to take place, which is $n_{X_i}^c = 4.12 \times 10^{-15} \text{ GeV}^3$. Thus, the LSPs will quickly annihilate (in less than a Hubble time) and the final abundance will be given by the critical value.

Thus, the relic density coming from the decay of the light moduli is given by

$$\begin{aligned} \Omega_{LSP} &= \frac{m_{LSP} Y_{LSP}^c s_0}{\rho_c}, \\ &= 0.26 h^{-2} \left(\frac{m_{LSP}}{100 \text{ GeV}} \right)^3 \left(\frac{10.75}{g_*(T_r)} \right)^{1/4} \left(\frac{3.26 \times 10^{-3} \text{ GeV}^{-2}}{\sigma_0} \right) \left(\frac{4}{D_{X_i}} \right)^{1/2} \left(\frac{2 m_{3/2}}{m_{X_i}} \right)^{3/2} \left(\frac{100 \text{ TeV}}{m_{3/2}} \right)^{3/2} \end{aligned} \quad (\text{A.29})$$

where s_0 and ρ_c are the entropy density and critical density today respectively, and we have used the experimental value $\rho_c/s_0 = 3.6 \times 10^{-9} h^2 \text{ GeV}$ where h parametrizes the Hubble parameter today with median value $h = 0.71$.

B. Couplings and Decay Widths of the Moduli and Meson Fields

In this section, we discuss the moduli couplings to MSSM particles and then calculate their decay widths in terms of the microscopic parameters of the G_2 -MSSM framework. This will motivate the benchmark values used for numerical results throughout the paper. We will find that the moduli decay into scalars is very important.

B.1 Moduli Couplings

Let us first consider the couplings associated with N eigenstates X_j of the geometric moduli s_i . For simplicity, we neglect the small mixing with the meson modulus ϕ (we will return to that later).

First consider the moduli coupling to gauge bosons through the gauge kinetic function f^{sm} . The relevant term is:

$$\mathcal{L} \supset -\frac{1}{4}\text{Im}(f_{sm})F_{\mu\nu}^a F^{a\mu\nu} \quad (\text{B.1})$$

$$= -\frac{1}{4}\langle\text{Im}(f_{sm})\rangle F_{\mu\nu}^a F^{a\mu\nu} - \frac{1}{4}\sum_i N_i^{sm}\delta s_i F_{\mu\nu}^a F^{a\mu\nu} \quad (\text{B.2})$$

where we have expanded the moduli as $s_i = \langle s_i \rangle + \delta s_i$. After normalizing the gauge fields and the moduli fields, the interaction term can be written as:

$$\mathcal{L}_{X_j gg} = \frac{1}{4f_{sm}}\sum_{i=1}^N N_i^{sm}\sqrt{\frac{2\langle s_i \rangle}{3a_i}}U_{ij}X_j F_{\mu\nu}^a F^{a\mu\nu} \quad (\text{B.3})$$

$$= \frac{\sqrt{7}}{6\sqrt{2}}\mathcal{B}\mathcal{C}_j X_j F_{\mu\nu}^a F^{a\mu\nu}, \quad (\text{B.4})$$

where \mathcal{B} and \mathcal{C}_j are defined as:

$$\mathcal{B} \equiv \left(\sum_{i=1}^N \frac{N_i^{sm}}{N_i} a_i \right)^{-1} \quad (\text{B.5})$$

$$\mathcal{C}_j \equiv \sum_{i=1}^N \frac{N_i^{sm}}{N_i} (\vec{X}_N)_i (\vec{X}_j)_i. \quad (\text{B.6})$$

For the heavy modulus, since $(X_N)_i^2 = \frac{3}{7}a_i$, we have $\mathcal{C}_N = \frac{3}{7}\mathcal{B}^{-1}$ while for the light moduli $X_i, i = 1, \dots, (N-1)$, it is easy to show:

$$\sum_{i=1}^{N-1} \mathcal{C}_i^2 = l^2 \sin^2 \theta, \quad (\text{B.7})$$

where l is the length of the vector \vec{X}'_N defined as $(\vec{X}'_N)_i \equiv (\vec{X}_N)_i N_i^{sm}/N_i$ and θ is the angle between \vec{X}'_N and \vec{X}_N . So, generically \mathcal{C}_i are less than one. There are two extreme cases: one when $N_i^{sm} = kN_i$ in which the moduli couplings to gauge bosons vanish since the vector \vec{X}_N is orthogonal to \vec{X}'_j , and the other when \vec{X}'_N equal to one of the X_i 's in which all \mathcal{C}_i 's are zero except one.

For the couplings to gauginos, the dominant contribution comes from the following terms in the lagrangian:

$$\mathcal{L} \supset -\frac{i}{4}\partial_i f_{sm} F^i \lambda^a \lambda^a + h.c. \quad (\text{B.8})$$

where $\partial_i f_{sm} = N_i^{sm}$ and $-i$ arises because of the convention of the moduli chiral fields $z_i = t_i + is_i$ we used. Expanding the F -terms of the moduli fields around their *vevs*, we have:

$$F^i = \langle F^i \rangle + \langle \partial_{s_k} F^i \rangle \delta s_k \quad (\text{B.9})$$

The derivative of the F -term can be calculated as follows:

$$\begin{aligned} \partial_{s_k} F^i &= \partial_{s_k} \left(e^{K/2} K^{i\bar{j}} (K_{\bar{j}} W^* + W_{\bar{j}}^*) \right) \\ &= -ie^{-i\gamma} m_{3/2} \left(\frac{4}{3} \frac{a_i}{N_i} N_k \nu^2 \frac{\tilde{z}}{\tilde{x}} + \frac{4}{3} \frac{N_k}{N_i} (3a_i - 2\delta_{ik}) \nu \frac{\tilde{y}}{\tilde{x}} + \frac{N_k}{N_i} (3a_i - 2\delta_{ik}) \right) \\ &= -ie^{-i\gamma} m_{3/2} \left(-\frac{4}{3} s_i N_k b_1 b_2 \nu - 3 \frac{N_k}{N_i} a_i + 2\delta_{ik} + \dots \right) \end{aligned} \quad (\text{B.10})$$

where in the last line, the subleading terms are not explicitly shown. γ is the phase in the superpotential which will be set to zero for simplicity without affecting any result here. We have used the following equations:

$$\partial_{s_i} K = -\frac{3a_i}{s_i}, \quad K^{i\bar{j}} = \frac{4s_i^2}{3a_i} \delta_{i\bar{j}}, \quad \partial_{s_k} K^{i\bar{j}} = \frac{2}{s_k} K^{i\bar{j}} \delta_{ik} \quad (\text{B.11})$$

After normalizing the moduli fields and the gauge fields, the couplings are given by:

$$\begin{aligned} \mathcal{L}_{X_i \lambda \lambda} &\approx \frac{1}{4} \sqrt{\frac{2}{3}} m_{3/2} \left[\left(\frac{4}{3} \nu^2 b_1 b_2 \right) \sum_{k=1}^N a_k^{1/2} U_{ki} - \frac{1}{f_{\text{sm}}} 2\nu \sum_{k=1}^N \frac{N_k^{sm}}{N_k} a_k^{1/2} U_{ki} \right] X_i \lambda^a \lambda^a + h.c. \\ &= \frac{\sqrt{14}}{12} m_{3/2} \left[\frac{4}{3} \nu^2 b_1 b_2 (\vec{X}_N \cdot \vec{X}_i) - 2\mathcal{B} (\vec{X}'_N \cdot \vec{X}_i) \right] X_i \lambda^a \lambda^a + h.c. \end{aligned} \quad (\text{B.12})$$

For the light moduli fields, the first term vanishes and the couplings turn out to be:

$$\mathcal{L}_{X_i \lambda \lambda} \approx -\frac{\sqrt{14}}{6} \mathcal{B} \mathcal{C}_i m_{3/2} X_i \lambda^a \lambda^a + h.c. \quad (\text{B.13})$$

For the heavy modulus field, the first dot product is unity and the coupling is:

$$\mathcal{L}_{X_i \lambda \lambda} \approx \frac{\sqrt{14}}{12} m_{3/2} \left(\frac{4}{3} \nu^2 b_1 b_2 \right) X_i \lambda^a \lambda^a + h.c. \quad (\text{B.14})$$

The moduli couplings to other MSSM particles can be derived generically by expanding all the moduli around their *vevs* in the supergravity lagrangian:

$$\mathcal{L} \supset \tilde{K}_{\bar{\alpha}\beta} \mathcal{D}_\mu \tilde{f}^{*\bar{\alpha}} \mathcal{D}^\mu \tilde{f}^\beta + i \tilde{K}_{\bar{\alpha}\beta} f^{\dagger\bar{\alpha}} \bar{\sigma}^\mu \mathcal{D}_\mu f^\beta - V(\tilde{f}^*, \tilde{f}) + \dots \quad (\text{B.15})$$

where f^α and \tilde{f}^α are fermions and their superpartners. The other derivative terms involving moduli and matter fields are not explicitly shown for simplicity. The relevant coupling here are the moduli-fermion-fermion coupling and the moduli-fermion-fermion coupling. They are found to be

$$\mathcal{L} \supset \partial_{s_i} \tilde{K}_{\bar{\alpha}\beta} \left[\delta s_i \partial_\mu \tilde{f}^{*\bar{\alpha}} \partial^\mu \tilde{f}^\beta + i \delta s_i f^{\dagger\bar{\alpha}} \bar{\sigma}^\mu \partial_\mu f^\beta \right] - \partial_{s_i} m'^2_{\bar{\alpha}\beta} \delta s_i \tilde{f}^{*\bar{\alpha}} \tilde{f}^\beta + \dots \quad (\text{B.16})$$

$$= g'^\alpha_{X_i \tilde{f} \tilde{f}} \left[\partial_\mu (X_i \tilde{f}_c^{*\bar{\alpha}}) \partial^\mu \tilde{f}_c^\alpha + c.c. + i X_i \tilde{f}_c^{\bar{\alpha}} \bar{\sigma}^\mu \partial_\mu f_c^\alpha \right] - g^\alpha_{X_i \tilde{f} \tilde{f}} X_i \tilde{f}_c^{*\bar{\alpha}} \tilde{f}_c^\alpha + \dots \quad (\text{B.17})$$

where \tilde{f}_c^α and f_c^α are the canonical normalized fields. For simplicity, we consider the Kahler metric to be diagonal $\tilde{K}_{\bar{\alpha}\beta} = \tilde{K}_\alpha \delta_{\bar{\alpha}\beta}$, then

$$\begin{aligned} g^\alpha_{X_j \tilde{f} \tilde{f}} &\approx m_{3/2}^2 \partial_{s_i} \log(\tilde{K}_\alpha) \sqrt{\frac{2s_i^2}{3a_i}} U_{ij} \\ &= \frac{\sqrt{14}}{3} m_{3/2}^2 (\vec{X}_N'')^\alpha \cdot \vec{X}_j \end{aligned} \quad (\text{B.18})$$

$$g'^\alpha_{X_j \tilde{f} \tilde{f}} = \frac{\sqrt{14}}{6} (\vec{X}_N'')^\alpha \cdot \vec{X}_j \quad (\text{B.19})$$

where $(\vec{X}_N'')^\alpha \equiv \xi_{i,\alpha} (X_N)_i / a_i$ and $\xi_{i,\alpha} \equiv s_i \partial_{s_i} \log(K_\alpha)$. In this calculation, we have used the fact that $\partial_{\phi_0} \tilde{K}_\alpha = 0$ and have neglected terms involving F -terms of geometric moduli F^i which are suppressed relative to $m_{3/2}$.

For the couplings to the higgs doublets, there are differences from other scalars. The kinetic terms and the mass terms for the higgs fields in the MSSM can be written as:

$$\begin{aligned} \mathcal{L} &\supset \tilde{K}_{H_u} \left[\partial_\mu H_u^* \partial^\mu H_u + i \tilde{H}_u \bar{\sigma}^\mu \partial_\mu \tilde{H}_u \right] + \dots \\ &- (\tilde{K}_{H_d}^{-1} |\mu'|^2 + m'^2_{H_u}) H_u^* H_u + (H_u \leftrightarrow H_d) \\ &- (B\mu' H_d H_u + c.c.) \end{aligned} \quad (\text{B.20})$$

where

$$\mu' = m_{3/2}Z - \bar{F}^{\bar{m}}\partial_{\bar{m}}Z \quad (\text{B.21})$$

is only generated by the higgs bilinear term in the Kahler potential [39]. To derive the modular couplings to higgs doublets, one needs $\partial_{s_i}\mu'$, which is:

$$\partial_{s_i}\mu' = (\partial_{s_i}m_{3/2})Z + m_{3/2}\partial_{s_i}Z - (\partial_{s_i}\bar{F}^{\bar{m}})\partial_{\bar{m}}Z - \bar{F}^{\bar{m}}\partial_{s_i}\partial_{\bar{m}}Z \quad (\text{B.22})$$

One can see that the second and the third terms are of order $m_{3/2}$ while the rest are suppressed. Therefore, the dominant contribution is:

$$\partial_{s_i}\mu' \approx \frac{1}{2}m_{3/2}(\partial_{s_m}Z) \left(-\frac{4}{3}s_m N_i b_1 b_2 \nu + 4\delta_{im} \right) \quad (\text{B.23})$$

For simplicity, taking all the phases of the superpotential and that of Z to be vanishing, we find:

$$\begin{aligned} -\mathcal{L} &\supset g_{X_j H_u H_u} X_j H_u^* H_u \quad (\text{B.24}) \\ g_{X_j H_u H_u} &\approx m_{3/2}^2 \left[Z_{\text{eff}}^2 \partial_{s_m} \log Z \left(-\frac{4}{3}s_m N_i b_1 b_2 \nu + 4\delta_{im} \right) - Z_{\text{eff}}^2 \partial_{s_i} \log \tilde{K}_{H_d} \right. \\ &\quad \left. + \partial_{s_i} \log \tilde{K}_{H_u} \right] \sqrt{\frac{2s_i^2}{3a_i}} U_{ij} \\ &= \frac{\sqrt{14}}{3} m_{3/2}^2 Z_{\text{eff}}^2 \left(-\frac{4}{3}\nu^2 b_1 b_2 \left(\sum_{m=1}^N \zeta_m \right) \vec{X}_N \cdot \vec{X}_j + 4\vec{X}_N''' \cdot \vec{X}_j \right. \\ &\quad \left. - (\vec{X}_N'')^{H_d} \cdot \vec{X}_j \right) + \frac{\sqrt{14}}{3} m_{3/2}^2 (\vec{X}_N'')^{H_u} \cdot \vec{X}_j \quad (\text{B.25}) \end{aligned}$$

where $(\vec{X}_N''')_i \equiv \frac{\zeta_i}{a_i}(X_N)_i$ and $\zeta_i \equiv s_i \partial_{s_i} \log(Z)$. We also use the fact that $\partial_{\phi_0} Z = 0$ and the F -terms $F_i/m_p \ll m_{3/2}$ for geometric moduli. To get the corresponding couplings for H_d , we can simply replace H_u by H_d in the above equations. The coupling of moduli to higgs through the kinetic term is similar to the non-higgs scalar

$$g'_{X_i H_u H_u}{}^\alpha = \frac{\sqrt{14}}{6} (\vec{X}_N'')^{H_u} \cdot \vec{X}_i \quad (\text{B.26})$$

Let us now consider the $B\mu$ term, which is given by:

$$\begin{aligned} B\mu' &= (2m_{3/2}^2 + V_0)Z - m_{3/2}\bar{F}^{\bar{m}}\partial_{\bar{m}}Z + m_{3/2}F^m[\partial_m Z - \partial_m \log(\tilde{K}_{H_u}\tilde{K}_{H_d})Z] \\ &\quad - \bar{F}^{\bar{m}}F^{\bar{n}}[\partial_{\bar{m}}\partial_{\bar{n}}Z - \partial_{\bar{n}}\log(\tilde{K}_{H_u}\tilde{K}_{H_d})\partial_{\bar{m}}Z]. \quad (\text{B.27}) \end{aligned}$$

The corresponding derivative is given by:

$$\partial_{s_i}B\mu' \approx \frac{1}{2}m_{3/2}^2 Z \partial_{s_i} \log(\tilde{K}_{H_u}\tilde{K}_{H_d}) \left(-\frac{4}{3}s_i N_k b_1 b_2 \nu + 2\delta_{ik} \right) + 2m_{3/2}^2 \partial_{s_i} Z, \quad (\text{B.28})$$

which gives rise to the coupling:

$$-\mathcal{L} \supset g_{X_j H_d H_u} X_j H_d H_u + c.c. \quad (\text{B.29})$$

$$\begin{aligned} g_{X_j H_d H_u} &\approx \frac{\sqrt{14}}{6} m_{3/2}^2 Z_{\text{eff}} \left(-\frac{4}{3}\nu^2 b_1 b_2 \left(\sum_{m=1}^N \xi_m^{H_u} \right) \vec{X}_N \cdot \vec{X}_j \right. \\ &\quad \left. + 2(\vec{X}_N'')^{H_u} \cdot \vec{X}_j + (H_u \rightarrow H_d) + 4\vec{X}_N''' \cdot \vec{X}_j \right) \quad (\text{B.30}) \end{aligned}$$

Besides the term mentioned above there is another coupling from the bilinear term in the kähler potential $K \sim Z(s_i)H_d H_u + h.c.$ [40]. This term leads to a coupling:

$$\mathcal{L} \supset g'_{X_j H_d H_u} \partial_\mu X_j \partial^\mu (H_d H_u) + c.c. \quad (\text{B.31})$$

$$g'_{X_j H_d H_u} = \frac{\sqrt{14}}{6} Z_{\text{eff}} \vec{X}'_N \cdot \vec{X}_j \quad (\text{B.32})$$

This coupling could be very important since it is proportional to the moduli mass squared if equations of motion of X_i are used. Again for the coupling to be unsuppressed, the bilinear coefficient Z should have a sizable dependence on the geometric moduli s_i , which is natural. This coupling is essential for electroweak symmetry breaking in the G_2 -MSSM.

B.2 Meson Couplings

In the G_2 -MSSM framework, the hidden sector is not sequestered from the visible sector and there are couplings between the hidden sector meson field ϕ and various MSSM particles, which we want to compute. First since the tree level gauge kinetic function does not depend on ϕ , there is no coupling to gauge bosons. However there are couplings to the gauginos which depend on ∂_{ϕ_0} , which are computed to be

$$\partial_{\phi_0} F^i = -ie^{-i\gamma} \frac{4s_i}{3\phi_0} \mathcal{F} m_{3/2}, \quad (\text{B.33})$$

$$\mathcal{F} = \frac{2QP_{\text{eff}}}{21P} + 2 + \frac{3}{P} + \mathcal{O}(P_{\text{eff}}^{-1}). \quad (\text{B.34})$$

After normalization of fields, the coupling of meson to the gauginos is given by:

$$\mathcal{L}_{\delta\phi_0\lambda\lambda} = e^{-i\gamma} \frac{1}{3\sqrt{2}\phi_0} \mathcal{F} m_{3/2} \delta\phi_0 \lambda\lambda \quad (\text{B.35})$$

We now move on to the couplings of the meson field to scalars. We will assume that the Kähler metric and the higgs bilinear Z do not depend on ϕ_0 . We then have for the non-higgs scalars:

$$\begin{aligned} \mathcal{L}_{\delta\phi_0\tilde{f}\tilde{f}} &= \frac{1}{\sqrt{2}\tilde{K}_\alpha} \frac{\partial m_\alpha'^2}{\partial\phi_0} \delta\phi_0 \tilde{f}^* \tilde{f} \\ &= \sqrt{2} m_{3/2} (\partial_{\phi_0} m_{3/2}) \delta\phi_0 \tilde{f}^* \tilde{f} \\ &\approx \sqrt{2} m_{3/2}^2 \phi_0 \left(1 + \frac{2}{3\phi_0^2}\right) \delta\phi_0 \tilde{f}^* \tilde{f} \end{aligned} \quad (\text{B.36})$$

In the above, we have neglected terms proportional to F_i/m_p which are $\ll m_{3/2}$. There are various kinds of couplings of the meson to the Higgs fields H_u and H_d . The coupling originating from the term $\int d^4\theta (ZH_u H_d + c.c)$ does *not* give rise to any contribution since Z is assumed to be independent of ϕ_0 . The couplings $\mathcal{L}_{\delta\phi_0 H_u^* H_u}$ and $\mathcal{L}_{\delta\phi_0 H_d^* H_d}$ are computed as follows:

$$\begin{aligned} \mathcal{L}_{\delta\phi_0 H_u H_u} &= g_{\delta\phi_0 H_u H_u} \delta\phi_0 \tilde{H}_u^* \tilde{H}_u \\ g_{\delta\phi_0 H_u H_u} &= \frac{1}{\sqrt{2}\tilde{K}_{H_u}} \frac{\partial(\tilde{K}_{H_d}^{-1} |\mu'|^2 + m_{H_u}^2)}{\partial\phi_0} \\ &\approx \sqrt{2}(Z_{\text{eff}}^2 + 1) m_{3/2}^2 \phi_0 \left[\left(1 + \frac{2}{3\phi_0^2}\right) + \left(\frac{Z_{\text{eff}}^2}{Z_{\text{eff}}^2 + 1}\right) \frac{2\mathcal{F}}{3\phi_0^2} \sum_{i=1}^N \zeta_i \right] \end{aligned} \quad (\text{B.37})$$

$\mathcal{L}_{\delta\phi_0\hat{H}_d^*\hat{H}_d}$ can be obtained from the above by replacing H_u with H_d . Again, we have neglected terms proportional to F_i/m_p . Finally, we look at the coupling $\mathcal{L}_{\delta\phi_0 H_d H_u}$. It is given by:

$$\begin{aligned}\mathcal{L}_{\delta\phi_0 H_d H_u} &= g_{\delta\phi_0 H_d H_u} \delta\phi_0 \tilde{H}_d \tilde{H}_u \\ g_{\delta\phi_0 H_d H_u} &= \frac{1}{\sqrt{2}(\tilde{K}_{H_u} \tilde{K}_{H_d})^{1/2}} \frac{\partial(B\mu')}{\partial\phi_0} \\ &\approx \sqrt{2} m_{3/2}^2 \phi_0 Z_{\text{eff}} \left[2\left(1 + \frac{2}{3\phi_0^2}\right) + \frac{\mathcal{F}}{3\phi_0^2} \sum_{i=1}^N (\xi_i^{H_u} + \xi_i^{H_d}) \right]\end{aligned}\quad (\text{B.38})$$

The coupling $\mathcal{L}_{\delta\phi_0 H_u^* H_d^*}$ can be computed by taking the complex conjugate of the above expression.

B.3 RG evolution of the couplings

In the last subsection, we computed all the relevant couplings of the moduli and meson at a high scale, presumably around the unification scale. However, since the scale at which moduli decay is much smaller than the unification scale, one should in principle use the effective couplings at that scale to compute the decay widths. The RG running of the moduli-scalar-scalar couplings are especially important for the third generation squarks and the higgs doublets and are the main focus of this subsection. The leading contribution to the β functions are terms proportional to $|y_t|^2$ and g_3^{210} , which are given below:

$$\begin{aligned}\beta(g_{X_j H_d H_u}) &\approx \frac{1}{16\pi^2} 3|y_t|^2 g_{X_j H_d H_u}, \\ \beta(g'_{X_j H_d H_u}) &\approx \frac{1}{16\pi^2} 3|y_t|^2 g'_{X_j H_d H_u}, \\ \beta(g_{X_j H_u H_u}) &\approx \frac{1}{16\pi^2} 6|y_t|^2 (g_{X_j H_u H_u} + X_t), \\ \beta(g'_{X_j H_u H_u}) &\approx \frac{1}{16\pi^2} 6|y_t|^2 g'_{X_j H_u H_u}, \\ \beta(g_{X_j \bar{Q}_3 \bar{Q}_3}) &\approx \frac{1}{16\pi^2} \left[g_{X_j \bar{Q}_3 \bar{Q}_3} \left(2|y_t|^2 - \frac{16}{3} g_3^2 \right) + 2|y_t|^2 X_t \right], \\ \beta(g'_{X_j \bar{Q}_3 \bar{Q}_3}) &\approx \frac{1}{16\pi^2} g'_{X_j \bar{Q}_3 \bar{Q}_3} \left(2|y_t|^2 - \frac{16}{3} g_3^2 \right), \\ \beta(g_{X_j \bar{u}_3 \bar{u}_3}) &\approx \frac{1}{16\pi^2} \left[g_{X_j \bar{u}_3 \bar{u}_3} \left(8|y_t|^2 - \frac{16}{3} g_3^2 \right) + 4|y_t|^2 X_t \right], \\ \beta(g'_{X_j \bar{u}_3 \bar{u}_3}) &\approx \frac{1}{16\pi^2} g'_{X_j \bar{u}_3 \bar{u}_3} \left(8|y_t|^2 - \frac{16}{3} g_3^2 \right),\end{aligned}\quad (\text{B.39})$$

where $X_t \equiv g_{X_j H_u H_u} + g_{X_j \bar{Q}_3 \bar{Q}_3} + g_{X_j \bar{u}_3 \bar{u}_3}$. For other beta functions not listed above, the RGE effects can be neglected.

To examine the RG effects on the moduli-scalar-scalar couplings, we take all the weighted dot products involved in the moduli-scalar-scalar couplings to be equal for simplicity¹¹,

$$\vec{X}_N''' \cdot \vec{X}_i = (\vec{X}_N'')^\alpha \cdot \vec{X}_i = \text{II}.\quad (\text{B.40})$$

¹⁰Here we have not included the digrams proportional to $g_{X_j gg}$ and $g_{X_j \bar{g}\bar{g}}$, since their contributions are relatively smaller

¹¹The more general case will be studied later.

This is reasonable as their structure is very similar. So the high scale couplings can be written as:

$$g_{X_j H_u H_u} = g_{X_j H_d H_d} = \frac{\sqrt{14}}{3} m_{3/2}^2 (3Z_{\text{eff}}^2 + 1) \Pi \quad (\text{B.41})$$

$$g'_{X_j H_u H_u} = g'_{X_j H_d H_d} = \frac{\sqrt{14}}{6} \Pi \quad (\text{B.42})$$

$$g_{X_j H_d H_u} = \frac{4\sqrt{14}}{3} m_{3/2}^2 Z_{\text{eff}} \Pi \quad (\text{B.43})$$

$$g'_{X_j H_d H_u} = \frac{\sqrt{14}}{6} Z_{\text{eff}} \Pi \quad (\text{B.44})$$

Using the beta functions given in Eq.(B.39), we can see that at low scale $g_{X_j H_u H_u}$ is squashed because of the large yukawa couplings. Similarly $g_{X_j \tilde{Q}_3 \tilde{Q}_3}$ and $g_{X_j \tilde{u}_3 \tilde{u}_3}$ decrease significantly and become negative at low scales.

One important thing to compute for moduli decay to light higgs is the effective coupling $g_{X_j hh}^{\text{eff}}$, which can be written in terms of the couplings to higgs doublets

$$\begin{aligned} g_{X_i hh}^{\text{eff}} &= (g_{X_i H_u H_u} - 2m_h^2 g'_{X_i H_u H_u}) \cos^2 \alpha + (g_{X_i H_d H_d} - 2m_h^2 g'_{X_i H_d H_d}) \sin^2 \alpha \\ &\quad - (g_{X_i H_d H_u} - m_{X_i}^2 g'_{X_i H_d H_u}) \sin 2\alpha \end{aligned} \quad (\text{B.45})$$

where all the couplings involved should be evaluated at low scales and α is the higgs mixing angle. For the G_2 -MSSM, the higgs sector is almost in the ‘‘decoupling region’’, which implies $\alpha \approx \beta - \frac{\pi}{2}$. Now with universal boundary condition for the weighted dot products for concreteness and simplicity, the effective coupling of moduli to hh final state is given by:

$$g_{X_i hh}^{\text{eff}} \approx \frac{\sqrt{14}}{3} m_{3/2}^2 [(3Z_{\text{eff}}^2 + 1)(\sin^2 \alpha + K_1 \cos^2 \alpha) - 2K_2 Z_{\text{eff}} \sin(2\alpha)] \Pi \quad (\text{B.46})$$

where K_1 and K_2 are the RG factors. To estimate these factors, we take $y_t = 1$, $\alpha_{\text{unif}}^{-1} = 26.7$ and $Z_{\text{eff}} = 1.58$, which is the same as the first Benchmark G_2 -MSSM. Then, typically we find $K_1 \sim 0.2$ and $K_2 \sim 0.5$. For readers not familiar with the details of the G_2 -MSSM, it is helpful to know that generically $\tan \beta \sim 1$ and $Z_{\text{eff}} \sim 1.5$. For the effective coupling to third generation squarks, including the RG effects, we have:

$$g_{X_j \tilde{u}_3 \tilde{u}_3}^{\text{eff}} \approx g_{X_j \tilde{Q}_3 \tilde{Q}_3}^{\text{eff}} \sim \frac{\sqrt{14}}{3} m_{3/2}^2 \Pi \quad (\text{B.47})$$

where $g_{X_j \tilde{f} \tilde{f}}^{\text{eff}} \equiv g_{X_j \tilde{f} \tilde{f}} - m_{\tilde{f}}^2 g'_{X_j \tilde{f} \tilde{f}}$. From the above RGE results, we find that the couplings to the non-higgs scalars and higgs should be roughly of the same order because of the large radiative correction even when some of them are suppressed relative to the other at the high scale boundary. Therefore, if the couplings to scalars are large, then we should expect a significant branching ratio of the moduli to LSPs.

For the coupling of the meson field to scalars, the β functions are exactly the same. Similar to the analysis of light moduli, we introduce factors K_1 and K_2 to account for the RG effects on $g_{\phi H_u H_u}$ and $g_{\phi H_d H_u}$. Typically one has $K_1 \sim 0.25$ and $K_2 \sim 0.5$. From Eq.(B.37) and (B.36), we find the coupling $g_{\phi H_u H_u}$ is at least $Z_{\text{eff}}^2 \mathcal{F} \sim 30$ times larger than $g_{\phi \tilde{f} \tilde{f}}$ at the high scale. Because of this large coupling $g_{\phi H_u H_u}$, even if the couplings $g_{\phi \tilde{Q}_3 \tilde{Q}_3}$ and $g_{\phi \tilde{u}_3 \tilde{u}_3}$ are zero at the high scale, they can still be generated at the low scale, which is proportional to $g_{\phi H_u H_u}$ by a factor $K_3 \sim 0.1$.

B.4 Decay Rates of the Moduli

Now that we have computed all the the relevant couplings for moduli decay, we can proceed to compute the corresponding decay widths. In the following, we give the result of decay widths for

all the moduli, calculated from the two-body width formulae. There could be contribution from three-body decays, which is generally small because of the phase space. Although certain three-body decays, e.g. moduli to top quarks and higgs [8, 40] is relatively large, it is still comparatively small in the current framework compared to the two-body decay modes.

For light moduli $X_i, i = 1, \dots, (N - 1)$, the total decay width is

$$\Gamma(X_i) \equiv \frac{D_{X_i} m_{X_i}^3}{m_p^2} = \frac{7}{72\pi} \left(N_G \mathcal{A}_1^{X_i} + N_G \mathcal{A}_2^{X_i} + \mathcal{A}_3^{X_i} + \mathcal{A}_4^{X_i} \right) \frac{m_{X_i}^3}{m_p^2}, \quad (\text{B.48})$$

where $\mathcal{A}_1^{X_i}$, $\mathcal{A}_2^{X_i}$, $\mathcal{A}_3^{X_i}$ and $\mathcal{A}_4^{X_i}$ are the corresponding coefficients for the decays to gauge bosons gg , gauginos $\tilde{g}\tilde{g}$, non-higgs scalars $\tilde{f}\tilde{f}$ and light higgs bosons hh respectively. They are given by:

$$\mathcal{A}_1^{X_i} = \frac{1}{2} \left(\sum_{i=1}^N \frac{N_i^{sm}}{N_i} a_i \right)^{-2} (\vec{X}'_N \cdot X_i)^2, \quad (\text{B.49})$$

$$\mathcal{A}_2^{X_i} = \left(\frac{m_{3/2}^2}{2m_{X_i}^2} \right) \left(\sum_{k=1}^N \frac{N_k^{sm}}{N_k} a_k \right)^{-2} (\vec{X}'_N \cdot X_i)^2, \quad (\text{B.50})$$

$$\mathcal{A}_3^{X_i} \approx \sum_{\alpha=\tilde{t}_L, \tilde{t}_R, \tilde{b}_L} 3 \left(\frac{m_{3/2}^4}{m_{X_i}^4} \right) \left(1 - 4 \frac{m_{f_\alpha}^2}{m_{X_i}^2} \right)^{1/2} \Pi^2, \quad (\text{B.51})$$

$$\mathcal{A}_4^{X_i} \approx \left(\frac{m_{3/2}^4}{2m_{X_i}^4} \right) \left[(3Z_{\text{eff}}^2 + 1)(\sin^2 \alpha + K_1 \cos^2 \alpha) - 2K_2 Z_{\text{eff}} \sin(2\alpha) \right]^2 \Pi^2 \quad (\text{B.52})$$

Here, weighted dot products in the scalar couplings are assumed to be equal and are denoted as Π as in the last subsection. In addition, the RGE effects on the couplings are included. In the above result, the gaugino and gauge bosons are treated as massless. The two-body decay to the standard model fermions is suppressed by $(\frac{m_f}{m_{X_i}})^2 \ll 10^{-4}$, so it is neglected in our result; even the top quark contribution is small. For the decay to non-higgs scalars, naively there is a large kinematic suppression since these scalars have mass close to $m_{3/2}$. However, the RGE running significantly decreases the third generation squark mass at the scale much lower than the unification scale. In G_2 MSSM framework, the lightest stop is \tilde{t}_R which is about 4 times lighter than the gravitino. It, therefore, has a large contribution to the partial width. In addition, \tilde{Q}_3 (\tilde{b}_L and \tilde{t}_L) are also light enough such that they contribute to the decay width.

The above result for \mathcal{A} 's depend on the specific choices of the fundamental parameters, such as a_i , N_i and N_i^{sm} , through several weighted dot products of vectors \vec{X}'_N and \vec{X}_i . These quantities are different for different moduli. However from Eq.(B.7) they are constrained by:

$$\sum_{i=1}^N (\vec{X}'_N \cdot \vec{X}_i)^2 = |\vec{X}'_N|^2 \sin^2 \theta. \quad (\text{B.53})$$

Similar constraints apply for other products. From the above equation, one expects that on average

$$(\vec{X}'_N \cdot \vec{X}_i)^2 \sim \frac{1}{N-1} |\vec{X}'_N|^2 \sin^2 \theta \quad (\text{B.54})$$

which is suppressed by $1/(N - 1)$. It is obvious that this symmetric configuration is favored in cosmology. If one wants the moduli to decay before BBN, then the most dangerous modulus is the one with the smallest total decay width, which is bounded by the average width. This gives rise to a strong constraint on the geometry of the G_2 manifold, since the width is suppressed by the number of moduli N . In the following discussion, we will focus on this symmetric configuration.

In order to evaluate the decay width and the branching ratio, one needs to know the typical values of these weighted dot products of \vec{X}_N and \vec{X}_i . To do the estimation, we generate a set of fundamental parameters a_i , N_i , N_i^{sm} , ξ_i and ζ_i randomly with the following conditions:

$$\sum_{i=1}^N a_i = \frac{7}{3}, \quad 1 < N_i^{sm} < 2, \quad 2 < N_i < 6, \quad -1 < \xi_i < 0, \quad -1 < \zeta_i < 0. \quad (\text{B.55})$$

The above ranges are chosen based on constraints arising from the G_2 framework and our current understanding of the Kähler metric of visible matter fields in realistic constructions. We also impose the supergravity condition $V_7 > 1$ and volume of three-cycle $V_Q^{sm} \approx 26$. The ranges of N_i and N_i^{sm} are chosen such that the efficiency of the parameter generation is maximized when the above constraints are imposed. Due to our primitive understanding about the kähler metric, the modular weights (corresponding to ξ_i and ζ_i) are taken randomly in the allowed range. We plot the distribution for $\mathcal{B}^{-2}(\vec{X}'_N \cdot \vec{X}_i)^2$ and $(\vec{X}'''_N \cdot \vec{X}_i)^2$ in Fig.4, where we can see the typical values are 2×10^{-4} and 20. This result can be understood from the very rough estimate $(\vec{X}'_N \cdot \vec{X}_i) \sim \sqrt{a_i} \sim 1/\sqrt{N}$ and $(\vec{X}'''_N \cdot \vec{X}_i) \sim 1/\sqrt{a_i} \sim \sqrt{N}$. The distribution of $((\vec{X}'''_N)^\alpha \cdot \vec{X}_i)^2$ is expected to be about the same as $(\vec{X}'''_N \cdot \vec{X}_i)^2$, since they all have the same structure. However, one should be aware that all the weighted dot products are independent and so are not necessarily equal.

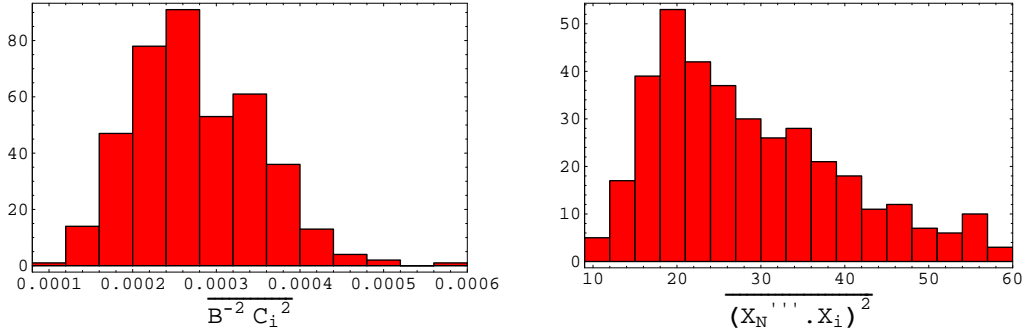


Figure 4: Left: distribution of the average of $\mathcal{B}^{-2}(\vec{X}'_N \cdot \vec{X}_i)^2$. Right: distribution of the average of the weighted dot product $(\vec{X}'''_N \cdot \vec{X}_i)^2$.

Now let us estimate the decay width for the light moduli. Consider the first benchmark model of G_2 -MSSM [39] for example, assuming the weighed dot products take their average value, we find $\mathcal{A}_1^{X_i} \approx \mathcal{A}_2^{X_i} \sim 10^{-4}$, $\mathcal{A}_3^{X_i} \sim 7.3$ and $\mathcal{A}_4^{X_i} \sim 20.5$. To summarize, the main channels of interest for light moduli decays and their partial widths are $\Gamma(gg) = \Gamma(\tilde{g}\tilde{g}) \approx 0.024 \text{ sec}^{-1}$, $\Gamma(\tilde{t}_R\tilde{t}_R) \approx 60 \text{ sec}^{-1}$, $\Gamma(\tilde{t}_L\tilde{t}_L) = \Gamma(\tilde{b}_L\tilde{b}_L) \approx 43 \text{ sec}^{-1}$ and $\Gamma(hh) \approx 412 \text{ sec}^{-1}$. The total width is the sum of these partial width. LSPs arise mainly from gauginos (including LSPs), $\tilde{t}\tilde{t}$ and $\tilde{b}\tilde{b}$, so the LSP branching ratio is the sum of the gaugino and squark channels divided by the total width. One can see that the decay to higgs and scalar dominate the decay of the light moduli. The total decay width is about 558 sec^{-1} or the corresponding $\mathcal{D}_{X_i} = 0.86$. The branching ratio of the light moduli to LSP is about 26%. These results should still be roughly correct for other benchmarks, differing at most by $\mathcal{O}(1)$ since the dependence on the mass spectrum is mild as seen from the explicit result of $\mathcal{A}_i^{X_i}$. The main uncertainty arises from the deviation of those weighted dot products from their typical values. To explore the more general case, one can relax the condition that all the weighted dot products are equal. Instead we choose:

$$\vec{X}'''_N \cdot \vec{X}_i = (\vec{X}''_N)^{H_u} \cdot \vec{X}_i = (\vec{X}''_N)^{H_d} \cdot \vec{X}_i = \Pi_1 \quad (\text{B.56})$$

$$(\vec{X}''_N)^{\tilde{Q}_3} \cdot \vec{X}_i = (\vec{X}''_N)^{\tilde{u}_3} \cdot \vec{X}_i = \Pi_2 \quad (\text{B.57})$$

Then we vary Π_1 and Π_2 according to the distributions of the weighted dot products in Fig.4. The distribution for D_{X_i} and the branching ratio to LSPs is shown in Fig.5. One can see that the branching ratio has a very small variation, but the distribution of D_{X_i} has a long tail. In the paper, we will use $0.4 < D_{X_i} < 4$ for concreteness, although other values may be possible.

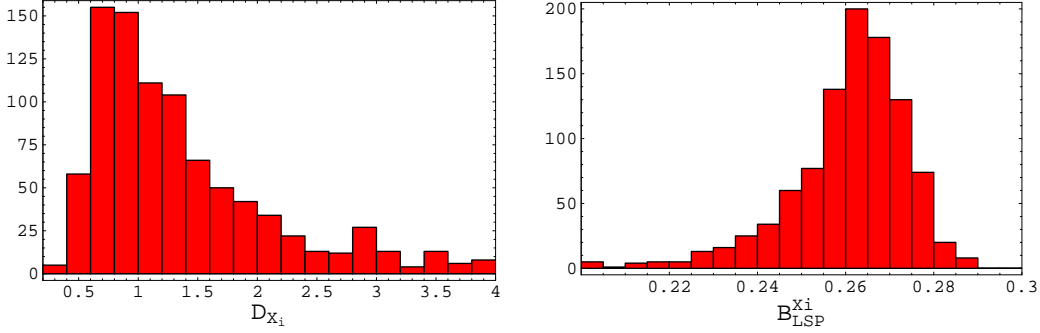


Figure 5: Left: distribution of D_{X_i} . Right: distribution of moduli branching ratio to LSP.

For the heavy modulus X_N , the total decay width is

$$\Gamma(X_N) = \frac{7}{72\pi} \left(N_G \mathcal{A}_1^{X_N} + N_G \mathcal{A}_2^{X_N} + \mathcal{A}_4^{X_N} \right) \frac{m_{X_N}^3}{m_p^2}, \quad (\text{B.58})$$

where $\mathcal{A}_i^{X_N}$ corresponds to the decay to gauge bosons gg , gauginos $\tilde{g}\tilde{g}$ and higgs bosons, and are given by

$$\mathcal{A}_1^{X_N} = \frac{9}{98} \quad (\text{B.59})$$

$$\mathcal{A}_2^{X_N} = \frac{2}{9} \left(\frac{m_{3/2}}{m_{X_N}} \right)^2 (\nu^2 b_1 b_2)^2 \quad (\text{B.60})$$

$$\mathcal{A}_4^{X_N} = Z_{\text{eff}}^2 \left(\vec{X}_N''' \cdot \vec{X}_i \right)^2. \quad (\text{B.61})$$

In the above result, we have not included the contributions from the decay to non-higgs scalars and fermions since they are suppressed by $(m_{3/2}/m_{X_N})^4$ and $(m_f/m_{X_N})^2$ given the large mass of the heavy modulus $m_{X_N} \sim 600 \times m_{3/2}$. Taking benchmark 1 of G_2 -MSSM in [39] and typical values for weighted dot products, we get $\mathcal{A}_1^{X_N} \approx 0.1$, $\mathcal{A}_2^{X_N} \approx 0.01$ and $\mathcal{A}_4^{X_N} \approx 50$. The total width is about $3 \times 10^{10} \text{ sec}^{-1}$ or the corresponding $D_{X_N} \approx 1.6$. The branching ratio to LSPs is about 3×10^{-3} .

The decays of moduli to gravitinos is also very important. The decay of a modulus to gravitinos can be calculated using the following formula: [19]

$$\Gamma(X \rightarrow 2\psi_{3/2}) \simeq \frac{|\mathcal{G}_X^{(eff)}|^2}{288\pi} \frac{m_X^5}{m_{3/2}^2 m_p^2} \quad (\text{B.62})$$

where $\mathcal{G}_X^{(eff)}$ is the effective coupling of the modulus field to gravitinos which includes effects of moduli mixing. For the heavy modulus, the coupling arises from the mixing with meson field, since the goldstino is mainly the fermionic partner of the meson. Since the heavy modulus is much heavier than the meson a rough estimate¹² gives $\mathcal{G}_X^{(eff)} \sim m_{3/2}/m_{X_N}$. Therefore, for the heavy

¹²There could be an additional suppression in special cases as discussed in [7, 12]. We thank Fuminobu Takahashi for discussions regarding this point.

modulus, the decay rate to gravitino is

$$\Gamma(X_N \rightarrow 2\psi_{3/2}) \sim \frac{1}{288\pi} \frac{m_{X_N}^3}{m_p^2} \quad (\text{B.63})$$

This corresponds to $B_{3/2}^{X_N} \sim 7 \times 10^{-4}$. In addition, since the heavy modulus decays much earlier than other moduli, the gravitino produced will be diluted by the subsequent moduli decays. So this estimate is enough for our discussion of gravitino problem. For both the light moduli and the meson fields, the decay to gravitino is kinematically suppressed since $m_{X_i}, m_{\phi_0} \approx 2m_{3/2}$.

B.5 Decay Width of the Meson

The total decay width of meson modulus is:

$$\Gamma(\delta\phi_0) \equiv \frac{D_\phi m_\phi^3}{m_p^2} = \frac{1}{72\pi} \left(N_G \mathcal{A}_1^{\phi_0} + \mathcal{A}_2^{\phi_0} + \mathcal{A}_3^{\phi_0} \right) \frac{m_\phi^3}{m_p^2}, \quad (\text{B.64})$$

where $\mathcal{A}_i^{\phi_0}$ corresponds to the decay to gauginos $\tilde{g}\tilde{g}$, non-higgs scalar $\tilde{f}\tilde{f}$ and light higgs bosons hh , and are given by:

$$\mathcal{A}_1^{\phi_0} = \frac{1}{2\phi_0^2} \mathcal{F}^2 \left(\frac{m_{3/2}}{m_\phi} \right)^2, \quad (\text{B.65})$$

$$\begin{aligned} \mathcal{A}_2^{\phi_0} &= \sum_\alpha 27\phi_0^2 K_3^2 Z_{\text{eff}}^4 \left((1 + Z_{\text{eff}}^{-2})(1 + \frac{2}{3\phi_0^2}) + \frac{2\mathcal{F}}{3\phi_0^2} \sum_{i=1}^N \zeta_i \right)^2 \\ &\quad \times \left(\frac{m_{3/2}^4}{m_\phi^4} \right) \left(1 - 4 \frac{m_{\tilde{f}_\alpha}^2}{m_\phi^2} \right)^{1/2}, \end{aligned} \quad (\text{B.66})$$

$$\begin{aligned} \mathcal{A}_3^{\phi_0} &= \frac{9}{2}\phi_0^2 \left(\frac{m_{3/2}^4}{m_{\phi_0}^4} \right) \left[Z_{\text{eff}}^2 \left((1 + Z_{\text{eff}}^{-2})(1 + \frac{2}{3\phi_0^2}) + \frac{2\mathcal{F}}{3\phi_0^2} \sum_{i=1}^N \zeta_i \right) (\sin^2 \alpha + K_1 \cos^2 \alpha) \right. \\ &\quad \left. - K_2 Z_{\text{eff}} \left(2(1 + \frac{2}{3\phi_0^2}) + \frac{\mathcal{F}}{3\phi_0^2} \sum_{i=1}^N (\xi_i^{H_u} + \xi_i^{H_d}) \right) \sin 2\alpha \right]^2. \end{aligned} \quad (\text{B.67})$$

Here, as discussed in the last subsection, the low scale couplings to third-generation squarks are dominantly generated from RG running and are related to the coupling $g_{\phi H_u H_u}$ by a factor $K_3 \sim 0.1$. For the first benchmark of G_2 -MSSM in [39] and taking the simplest assumption $\xi_i = \zeta_i = -1/2$, we get $\mathcal{A}_1^{\phi_0} \approx 13.7$, $\mathcal{A}_2^{\phi_0} \approx 2.9 \times 10^4$ and $\mathcal{A}_3^{\phi_0} \approx 1.3 \times 10^5$. One can see that this result is enhanced from the naive estimate by the total number of moduli $\sim N$ and large (hidden-sector) three-cycle volume ν . The total decay width is about $4.6 \times 10^5 \text{ sec}^{-1}$, corresponding to $D_\phi = 711$. The branching ratio to LSPs is about 18%. Again, this can change by $\mathcal{O}(1)$ for other benchmarks.

References

- [1] G. D. Coughlan, W. Fischler, E. W. Kolb, S. Raby and G. G. Ross, ‘‘Cosmological Problems For The Polonyi Potential,’’ Phys. Lett. B **131**, 59 (1983).
- [2] J. R. Ellis, D. V. Nanopoulos and M. Quiros, ‘‘On the Axion, Dilaton, Polonyi, Gravitino and Shadow Matter Problems in Supergravity and Superstring Models,’’ Phys. Lett. B **174**, 176 (1986).
- [3] B. de Carlos, J. A. Casas, F. Quevedo and E. Roulet, ‘‘Model independent properties and cosmological implications of the dilaton and moduli sectors of 4-d strings,’’ Phys. Lett. B **318**, 447 (1993) [arXiv:hep-ph/9308325].

- [4] T. Banks, D. B. Kaplan and A. E. Nelson, “Cosmological implications of dynamical supersymmetry breaking,” *Phys. Rev. D* **49**, 779 (1994) [arXiv:hep-ph/9308292].
- [5] S. Nakamura and M. Yamaguchi, “A Note on Polonyi Problem,” *Phys. Lett. B* **655**, 167 (2007) [arXiv:0707.4538 [hep-ph]].
- [6] M. Y. Khlopov and A. D. Linde, “Is It Easy To Save The Gravitino?,” *Phys. Lett. B* **138**, 265 (1984).
- [7] M. Dine, R. Kitano, A. Morisse and Y. Shirman, “Moduli decays and gravitinos,” *Phys. Rev. D* **73**, 123518 (2006) [arXiv:hep-ph/0604140].
- [8] M. Endo, M. Kawasaki, F. Takahashi and T. T. Yanagida, “Inflaton decay through supergravity effects,” *Phys. Lett. B* **642**, 518 (2006) [arXiv:hep-ph/0607170].
- [9] V. S. Rychkov and A. Strumia, “Thermal production of gravitinos,” *Phys. Rev. D* **75**, 075011 (2007) [arXiv:hep-ph/0701104].
- [10] M. Endo, K. Hamaguchi and F. Takahashi, “Moduli-induced gravitino problem,” *Phys. Rev. Lett.* **96**, 211301 (2006) [arXiv:hep-ph/0602061].
- [11] S. Nakamura and M. Yamaguchi, “Gravitino production from heavy moduli decay and cosmological moduli problem revived,” *Phys. Lett. B* **638**, 389 (2006) [arXiv:hep-ph/0602081].
- [12] M. Endo, K. Hamaguchi and F. Takahashi, “Moduli / inflaton mixing with supersymmetry breaking field,” *Phys. Rev. D* **74**, 023531 (2006) [arXiv:hep-ph/0605091].
- [13] M. Endo, F. Takahashi and T. T. Yanagida, “Anomaly-Induced Inflaton Decay and Gravitino-Overproduction Problem,” *Phys. Lett. B* **658**, 236 (2008) [arXiv:hep-ph/0701042];
- [14] M. Endo, F. Takahashi and T. T. Yanagida, “Inflaton Decay in Supergravity,” *Phys. Rev. D* **76**, 083509 (2007) [arXiv:0706.0986 [hep-ph]].
- [15] K. Ichikawa, M. Kawasaki and F. Takahashi, “The oscillation effects on thermalization of the neutrinos in the universe with low reheating temperature,” *Phys. Rev. D* **72**, 043522 (2005) [arXiv:astro-ph/0505395].
- [16] S. Nakamura and M. Yamaguchi, “Gravitino production from heavy moduli decay and cosmological moduli problem revived,” *Phys. Lett. B* **638**, 389 (2006) [arXiv:hep-ph/0602081].
- [17] T. Asaka, S. Nakamura and M. Yamaguchi, “Gravitinos from heavy scalar decay,” *Phys. Rev. D* **74**, 023520 (2006) [arXiv:hep-ph/0604132].
- [18] M. Endo, K. Hamaguchi and F. Takahashi, “Moduli-induced gravitino problem,” *Phys. Rev. Lett.* **96**, 211301 (2006) [arXiv:hep-ph/0602061].
- [19] M. Kawasaki, F. Takahashi and T. T. Yanagida, “The gravitino overproduction problem in inflationary universe,” *Phys. Rev. D* **74**, 043519 (2006) [arXiv:hep-ph/0605297].
- [20] M. Nagai and K. Nakayama, “Nonthermal dark matter in mirage mediation,” *Phys. Rev. D* **76**, 123501 (2007) [arXiv:0709.3918 [hep-ph]].
- [21] M. Endo and F. Takahashi, “Non-thermal production of dark matter from late-decaying scalar field at intermediate scale,” *Phys. Rev. D* **74**, 063502 (2006) [arXiv:hep-ph/0606075].
- [22] M. Kawasaki and K. Nakayama, “Baryon Asymmetry in Heavy Moduli Scenario,” *Phys. Rev. D* **76**, 043502 (2007) [arXiv:0705.0079 [hep-ph]].
- [23] S. Kachru, R. Kallosh, A. Linde and S. P. Trivedi, “De Sitter vacua in string theory,” *Phys. Rev. D* **68**, 046005 (2003) [arXiv:hep-th/0301240].
- [24] V. Balasubramanian, P. Berglund, J. P. Conlon and F. Quevedo, “Systematics of moduli stabilisation in Calabi-Yau flux compactifications,” *JHEP* **0503**, 007 (2005) [arXiv:hep-th/0502058].
- [25] J. P. Conlon, F. Quevedo and K. Suruliz, “Large-volume flux compactifications: Moduli spectrum and D3/D7 soft supersymmetry breaking,” *JHEP* **0508**, 007 (2005) [arXiv:hep-th/0505076].
- [26] M. R. Douglas and S. Kachru, “Flux compactification,” *Rev. Mod. Phys.* **79**, 733 (2007) [arXiv:hep-th/0610102].

- [27] M. P. Hertzberg, M. Tegmark, S. Kachru, J. Shelton and O. Ozcan, “Searching for Inflation in Simple String Theory Models: An Astrophysical Perspective,” *Phys. Rev. D* **76**, 103521 (2007) [arXiv:0709.0002 [astro-ph]].
- [28] L. McAllister and E. Silverstein, “String Cosmology: A Review,” *Gen. Rel. Grav.* **40**, 565 (2008) [arXiv:0710.2951 [hep-th]].
- [29] J. P. Conlon and F. Quevedo, “Astrophysical and Cosmological Implications of Large Volume String Compactifications,” *JCAP* **0708**, 019 (2007) [arXiv:0705.3460 [hep-ph]].
- [30] B. Acharya, “A Moduli Fixing Mechanism in M theory” arXiv:hep-th/0212294
- [31] C. Beasley and E. Witten, “A note on fluxes and superpotentials in M-theory compactifications on manifolds of $G(2)$ holonomy,” *JHEP* **0207**, 046 (2002) [arXiv:hep-th/0203061].
- [32] B. Acharya and E. Witten, “Chiral fermions from manifolds of $G(2)$ holonomy,” arXiv:hep-th/0109152.
- [33] E. Witten, “Anomaly cancellation on $G(2)$ manifolds,” arXiv:hep-th/0108165.
- [34] M. Atiyah and E. Witten, “M-theory dynamics on a manifold of $G(2)$ holonomy,” *Adv. Theor. Math. Phys.* **6**, 1 (2003) [arXiv:hep-th/0107177].
- [35] E. Witten, “Deconstruction, $G(2)$ holonomy, and doublet-triplet splitting,” arXiv:hep-ph/0201018.
- [36] T. Friedmann and E. Witten, “Unification scale, proton decay, and manifolds of $G(2)$ holonomy,” *Adv. Theor. Math. Phys.* **7**, 577 (2003) [arXiv:hep-th/0211269].
- [37] B. Acharya, K. Bobkov, G. Kane, P. Kumar and D. Vaman, “An M theory solution to the hierarchy problem,” *Phys. Rev. Lett.* **97**, 191601 (2006) [arXiv:hep-th/0606262].
- [38] B. S. Acharya, K. Bobkov, G. L. Kane, P. Kumar and J. Shao, “Explaining the electroweak scale and stabilizing moduli in M theory,” *Phys. Rev. D* **76**, 126010 (2007) [arXiv:hep-th/0701034].
- [39] B. S. Acharya, K. Bobkov, G. L. Kane, J. Shao and P. Kumar, “The G_2 -MSSM - An M Theory motivated model of Particle Physics,” arXiv:0801.0478 [hep-ph].
- [40] T. Moroi and L. Randall, “Wino cold dark matter from anomaly-mediated SUSY breaking,” *Nucl. Phys. B* **570**, 455 (2000) [arXiv:hep-ph/9906527].
- [41] M. Dine, L. Randall and S. D. Thomas, “Baryogenesis From Flat Directions Of The Supersymmetric Standard Model,” *Nucl. Phys. B* **458**, 291 (1996) [arXiv:hep-ph/9507453].
- [42] N. Kaloper and K. A. Olive, “Dilatons in string cosmology,” *Astropart. Phys.* **1**, 185 (1993).
- [43] R. Brustein, S. P. de Alwis and P. Martens, “Cosmological stabilization of moduli with steep potentials,” *Phys. Rev. D* **70**, 126012 (2004) [arXiv:hep-th/0408160].
- [44] R. Brustein and R. Madden, “Classical corrections in string cosmology,” *JHEP* **9907**, 006 (1999) [arXiv:hep-th/9901044].
- [45] G. Huey, P. J. Steinhardt, B. A. Ovrut and D. Waldram, “A cosmological mechanism for stabilizing moduli,” *Phys. Lett. B* **476**, 379 (2000) [arXiv:hep-th/0001112].
- [46] N. Kaloper, J. Rahmfeld and L. Sorbo, “Moduli entrapment with primordial black holes,” *Phys. Lett. B* **606**, 234 (2005) [arXiv:hep-th/0409226].
- [47] T. Battefeld and S. Watson, “String gas cosmology,” *Rev. Mod. Phys.* **78**, 435 (2006) [arXiv:hep-th/0510022].
- [48] S. Cremonini and S. Watson, “Dilaton dynamics from production of tensionless membranes,” *Phys. Rev. D* **73**, 086007 (2006) [arXiv:hep-th/0601082].
- [49] L. Kofman, A. Linde, X. Liu, A. Maloney, L. McAllister and E. Silverstein, “Beauty is attractive: Moduli trapping at enhanced symmetry points,” *JHEP* **0405**, 030 (2004) [arXiv:hep-th/0403001].
- [50] S. Watson, “Moduli stabilization with the string Higgs effect,” *Phys. Rev. D* **70**, 066005 (2004) [arXiv:hep-th/0404177].

- [51] B. Greene, S. Judes, J. Levin, S. Watson and A. Weltman, “Cosmological Moduli Dynamics,” *JHEP* **0707**, 060 (2007) [arXiv:hep-th/0702220].
- [52] M. Dine, Y. Nir and Y. Shadmi, “Enhanced symmetries and the ground state of string theory,” *Phys. Lett. B* **438**, 61 (1998) [arXiv:hep-th/9806124].
- [53] C. Vafa, “The string landscape and the swampland,” arXiv:hep-th/0509212.
- [54] R. Brustein and P. J. Steinhardt, “Challenges for superstring cosmology,” *Phys. Lett. B* **302**, 196 (1993) [arXiv:hep-th/9212049].
- [55] M. Dine and N. Seiberg, “Is The Superstring Weakly Coupled?,” *Phys. Lett. B* **162**, 299 (1985).
- [56] E. W. Kolb and M. S. Turner, “The Early universe,” *Front. Phys.* **69**, 1 (1990).
- [57] M. Kawasaki, K. Kohri and N. Sugiyama, “Cosmological Constraints on Late-time Entropy Production,” *Phys. Rev. Lett.* **82**, 4168 (1999) [arXiv:astro-ph/9811437].
- [58] G. F. Giudice, E. W. Kolb and A. Riotto, “Largest temperature of the radiation era and its cosmological implications,” *Phys. Rev. D* **64**, 023508 (2001) [arXiv:hep-ph/0005123].
- [59] M. Kawasaki, K. Kohri and N. Sugiyama, “MeV-scale reheating temperature and thermalization of neutrino background,” *Phys. Rev. D* **62**, 023506 (2000) [arXiv:astro-ph/0002127].
- [60] S. Hannestad, “What is the lowest possible reheating temperature?,” *Phys. Rev. D* **70**, 043506 (2004) [arXiv:astro-ph/0403291].
- [61] E. Komatsu *et al.* [WMAP Collaboration], “Five-Year Wilkinson Microwave Anisotropy Probe (WMAP) Observations:Cosmological Interpretation,” arXiv:0803.0547 [astro-ph].
- [62] I. Affleck and M. Dine, *Nucl. Phys. B* **249**, 361 (1985).
- [63] J. Simon, R. Jimenez, L. Verde, P. Berglund and V. Balasubramanian, “Using cosmology to constrain the topology of hidden dimensions,” arXiv:astro-ph/0605371.
- [64] V. Balasubramanian, P. Berglund, R. Jimenez, J. Simon and L. Verde, “Topology from Cosmology,” arXiv:0712.1815 [hep-th].
- [65] N. Arkani-Hamed, G. L. Kane, J. Thaler and L. T. Wang, “Supersymmetry and the LHC inverse problem,” *JHEP* **0608**, 070 (2006) [arXiv:hep-ph/0512190].